Studies of the dynamics of nuclear clustering in human syncytiotrophoblast

DOI:
10.1530/REP-15-0544

Document Version
Accepted author manuscript

Reproduction Advance Publication first posted on 21 March 2016 as Manuscript REP-15-0544

Studies of the dynamics of nuclear clustering in human syncytiotrophoblast

SJ Calvert[1,2], MS Longtine[3], S Cotter[4], CJP Jones[1,2], CP Sibley[1,2], JD Aplin[1,2], DM Nelson[3], and AEP Heazell[1,2]

1. Centre for Women's Health, Institute of Human Development, School of Medicine, University of Manchester, UK

2. Manchester Academic Health Science Centre, St. Mary's Hospital, Central Manchester University Hospitals NHS Foundation Trust, Manchester, UK

3. Department of Obstetrics and Gynecology, Washington University School of Medicine, St. Louis, Missouri, USA

4. School of Mathematics, Alan Turing Building, University of Manchester, Manchester, UK

Corresponding author: Dr Sarah Calvert

Email: s.j.calvert87@gmail.com

Address: Institute of Human Development, Faculty of Medical and Human Sciences, The University of Manchester, 5th Floor (Research), St Mary's Hospital, Oxford Road, Manchester, M13 9WL, UK

Short Title: Modelling nuclear clustering in the placenta

Abstract

Syncytial nuclear aggregates (SNAs), clusters of nuclei in the syncytiotrophoblast of the human placenta, are increased as gestation advances and in pregnancy pathologies. The origins of increased SNAs are unclear, but a better appreciation of mechanism may give insight into placental ageing and factors underpinning dysfunction. We developed three models to investigate whether SNA formation results from a dynamic process of nuclear movement and to generate alternative hypotheses. SNA count and size were measured in placental explants cultured over 16 days and particles released into culture medium were quantified. Primary trophoblasts were cultured for 6 days. Explants and trophoblasts were cultured with and without cytoskeletal inhibitors. An in silico model was developed to examine the effects of modulating nuclear behaviour on clustering. In explants, neither median SNA number (108 SNA/mm^2 villous area) nor size (283μm^2) changed over time. Subcellular particles from conditioned culture medium showed a wide range of sizes that overlapped with those of SNAs. Nuclei in primary trophoblasts did not change position relative to other nuclei; apparent movement was associated with positional changes of the syncytial cell membrane. In both models, SNAs and nuclear clusters were stable despite pharmacological disruption of cytoskeletal activity. In silico, increased nuclear movement, adhesiveness and sites of cytotrophoblast fusion were related to nuclear clustering. The prominence of SNAs in pregnancy disorders may not result from an active process involving cytoskeletal-mediated rearrangement of syncytial nuclei. Further insights into the mechanism(s) of SNA formation will aid understanding of their increased presence in pregnancy pathologies.

Introduction

The placenta is a transient organ, the correct development of which is essential for a healthy pregnancy. In the human placenta, the maternal surface of placental villi is covered by syncytiotrophoblast which is in direct contact with maternal blood. This essential cell layer performs many functions including gas exchange, hormone production, immune protection and the transport of nutrients from mother to fetus (Boyd and Hamilton, 1970). To allow growth of the placenta, subjacent mononucleate progenitor cells, cytotrophoblasts, replicate and fuse into the terminally differentiated syncytiotrophoblast (Boyd and Hamilton, 1967). Pregnancy disorders such as preeclampsia are characterised by abnormal placental development, alterations in trophoblast apoptosis and release of trophoblast-derived fragments into the maternal circulation (Chaddha *et al.*, 2004; Hahn *et al.*, 2005; Goswami *et al.*, 2006; Heazell *et al.*, 2008a).

In the syncytiotrophoblast, nuclei can cluster to form syncytial nuclear aggregates (SNAs). In vivo, SNAs accumulate throughout pregnancy; they are especially noted in histological analyses of prolonged pregnancies (post-term; >40 weeks, Jones and Fox 1978) but are found at earlier gestational ages and seen in greater abundance in pregnancies complicated by preeclampsia (Tenney and Parker, 1940; Al-Allaf *et al.*, 2008; Corrêa *et al.*, 2008; Calvert *et al.*, 2013). Similarly, in vitro, formation of SNAs is increased by oxidative stress (Heazell *et al.*, 2007) and culture of isolated trophoblast cells results in spontaneous fusion between 24-48 hours (h) (Kliman *et al.*, 1986), with the possibility that the nuclei will cluster, here termed syncytial nuclear clusters (SNCs).

Syncytial knots, a subtype of SNA, form more towards term and in the past have often been thought to represent "aging" of the placenta. In contrast to syncytial knots other SNA subtypes, and more specifically syncytial sprouts, may reflect placental growth (Cantle *et al.*, 1987; Burton and Jones, 2009). The morphology of syncytial knots shows nuclei with dense heterochromatin. This nuclear condensation was previously thought to indicate a trajectory towards apoptosis (Huppertz *et al.*, 2006); however, we previously characterised SNAs in normal term placentas and demonstrated that most of the constituent nuclei are not apoptotic, although knots are more likely than other types of SNA to be apoptotic (Coleman *et al.*, 2013). Similarly, others have found little evidence that there are apoptotic changes in normal syncytiotrophoblast (Burton and Jones, 2009; Longtine *et al.*, 2012a).

Instead SNAs, and in particular syncytial knots, have been found to show epigenetic changes associated with oxidative damage that could lead to heterochromatin formation (Fogarty *et al.*, 2013), without necessary progression to apoptosis or shedding of apoptotic debris.

Despite the longstanding association between SNAs and pregnancy pathologies, unanswered questions remain. In a recent review, Mayhew proposed avenues for further investigation of SNAs (Mayhew, 2014) such as understanding why SNAs, including knots, form. Another avenue was to determine the benefits of allowing oxidative-damaged nuclei with condensed chromatin to accumulate, if SNAs are not preferentially extruded. Mayhew also raises questions about the relevance of increased density of SNAs to preeclampsia (Mayhew, 2014), in particular an increase in syncytial knots (Calvert *et al.*, 2013). The mechanism of SNA formation remains unknown (Aplin, 2010) but cytoskeletal proteins are found in association with them (Jones and Fox, 1977; Coleman *et al.*, 2013). As actin microfilaments and microtubules are involved in nuclear movement and anchorage in syncytia of skeletal muscle, *Danio rerio* and *Caenorhabditis elegans* development (Malone *et al.*, 1999; Frock *et al.*, 2006; Carvalho *et al.*, 2009), we hypothesised they could be involved in SNA formation in human syncytiotrophoblast.

Our objectives for this study were to: 1) use placental villous explant cultures to examine the dynamics of SNAs. 2) Use primary trophoblast cells in vitro to observe the formation of syncytial nuclear clusters (SNCs, the form we identified SNAs take in cell culture). 3) Explore cytoskeletal disruption in these models to see if this affects SNA or SNC numbers, giving insight on whether SNAs are formed or held together using dynamic cytoskeletal rearrangements. Lastly, 4) use data obtained from these in vitro models to develop an in silico model of nuclear clustering to explore factors which may influence the formation and maintenance of SNAs or SNCs. To address objectives 1 and 2, this study extended the length of in vitro culture from that typically employed, as estimates suggest that de novo synthesis of SNAs could take weeks (Huppertz *et al.*, 2002, 2003) and that SNC formation would occur in more mature syncytia. Consequently, an assessment of viability was conducted prior to experiments to disrupt the cytoskeleton. The effect of pharmacological agents was examined in the cultured trophoblast model at two time points: i) after SNCs were thought to have formed at 72h and ii) during syncytialisation at 40-42h. In placental explants, it was anticipated that SNAs would develop

from existing nuclei during culture, therefore pharmacological agents were added after 24h as previous experiments altering culture conditions at this time had an effect on SNAs (Heazell *et al.*, 2007).

Methods

Placental collection, tissue and cell culture

All reagents were purchased from Sigma-Aldrich (Poole, UK for explant work and St. Louis, USA for cell preparations) unless otherwise stated. Placentas used for explant work were obtained under tissue biobank ethics from St. Mary's Hospital Maternity Unit (Manchester, UK) following informed consent, approved by North West (Haydock Park) Research Ethics Committee (Ref: 08/H1010/55). Placentas were selected if delivered after 37 weeks gestation and with no maternal or fetal morbidities during pregnancy (demographic information in supplementary table 1). Tissue processing was started within 30 minutes (min) of delivery; explants were made from three randomly selected areas of the placenta and cultured in medium using Netwells at the medium/gaseous interface, as previously described (Siman *et al.*, 2001). CMRL-1066 culture medium was supplemented with 10% fetal bovine serum, NaHCO3 (2.2mg/ml), penicillin G (100IU/ml), streptomycin sulphate (100µg/ml), L-glutamine (100µg/ml), retinol acetate (1µg/ml), insulin (1µg/ml) and hyaluronic acid (1µg/ml) (pH 7.2, Invitrogen, Life Technologies, Paisley, UK). Villous explants were cultured for up to 16 day (d), which was thought sufficient to enable the kinetics of aggregation and shedding to be observed as it has been hypothesised that SNAs form and are shed within 14-28d (Huppertz *et al.*, 2002, 2003). Normoxia for term placenta has been estimated to be between 6% and 13% oxygen (O_2) tension (Jauniaux *et al.*, 2000; Sullivan *et al.*, 2006; Heazell *et al.*, 2008b; Pringle *et al.*, 2010), however, cultured cells may take up gases more quickly than the gases can diffuse, meaning they are usually hypoxic (Metzen *et al.*, 1995; Pettersen *et al.*, 2005; Tuuli *et al.*, 2011; Chen *et al.*, 2013). Therefore, it was decided to culture explants at both 6% O_2 with 5% CO_2 and 89% N_2 and 20% O_2 with 5% CO_2 and 75% N_2. Explants were weighed and fixed for 24h in 10% neutral buffered formalin from fresh tissue and at d4, d8, d12 and d16 (n=6). Medium was changed daily, with conditioned medium collected and stored at -80°C.

For experiments with purified primary trophoblasts, placentas were collected under informed consent, approved by the Institutional Review Board of Washington University School of Medicine in St. Louis, MO. Normal term placentas of 38-40 weeks gestation (n=3) were obtained after uncomplicated Caesarean section. Primary trophoblast cells were isolated as described by Chen *et al.* (Chen *et al.*, 2006) and plated at a density of 200,000 cells/cm^2 to encourage an even, single layer for best visibility. Trophoblasts were cultured in a 5% CO_2/air environment at 37°C in DMEM supplemented with 10% fetal bovine serum (Invitrogen, Life Technologies, Grand Island, NY, USA), 20mM HEPES pH 7.4 (Sigma, St. Louis, MO USA), 100units/ml penicillin and 100 µg/ml streptomycin, for the times indicated, with daily changes of medium. As noted, selected experiments also received 100ng/ml Epidermal Growth Factor (EGF) (Millipore, Temecula, USA) added to cultures which has been suggested to increase the rate and extent of syncytiotrophoblast formation in vitro (Morrish *et al.*, 1987, 1997; Johnstone *et al.*, 2005) and to reduce trophoblast stress-induced apoptosis (Garcia-Lloret *et al.*, 1996; Moll *et al.*, 2007; Humphrey *et al.*, 2008).

Analysis of tissue viability and hormone release from syncytiotrophoblast

Tissue viability was assessed by lactate dehydrogenase (LDH) release using a cytotoxicity detection kit (Roche Applied Science, Mannheim, Germany) and production of the hormones human chorionic gonadotropin (hCG) and human placental lactogen, (hPL) into conditioned culture medium using kits hCG ELISA EIA-1469 (DRG International, Springfield, New Jersey, USA) and hPL ELISA EIA-1283 (DRG International) (Audette *et al.*, 2010). Also, proliferation and apoptosis were measured as previously described (Heazell *et al.*, 2008b).

Inhibition of intracellular motility

Explants (n=6) were cultured in 20% O_2 and treated after 24h with the following cytoskeletal disruptors, all from Sigma: cytochalasin D (actin polymerisation inhibitor), nocodazole (microtubule polymerisation inhibitor), paclitaxel (microtubule stabiliser) at 0.1mM, 1mM or 10mM or with solvent control (0.2% dimethyl sulfoxide (DMSO)) for 20h before washing and culturing the explants for a further 48h; treated explants were weighed and fixed at d4.

To assess SNC stability in cells, primary trophoblasts were cultured with EGF for 72h and then treated for 6h with either 10µM nocodazole, 1µM cytochalasin D, or both nocodazole and cytochalasin

D. Control cultures were treated with 0.2% DMSO. Additional experiments were conducted to examine whether SNC formation was inhibited by culturing primary trophoblasts for 40-42h before 18h treatment with drugs or control at the same concentrations as the other trophoblast experiments. After cytoskeletal disruptor treatments, primary trophoblasts were fixed for imaging.

Examination of shed particles

Explant conditioned culture medium was collected at 48h intervals for 16d and processed immediately (n=4). Medium was centrifuged at 9000*g* for 4min using MiniSpin (Eppendorf, UK). The pellet was resuspended in 200µl phosphate buffered saline (PBS) and stained with 4',6-diamidino-2-phenylindole (DAPI) and CellTracker Orange (Invitrogen, Life Technologies, Paisley, UK). Briefly, 0.1µl CellTracker Orange and 0.5µl DAPI were added for 10min at room temperature to stain all nuclei and cytoplasm, followed by centrifugation at 900*g* for 5min. The pellet was resuspended away from light, washed for 3min and centrifuged at 900*g* for 5min. The final pellet was resuspended in 100µl PBS and placed in a 96-well dish. Particle size and number were analysed using the BD Pathway Bioimager 855 High Content Screening System (BD Bioscience) and Image J 1.45s (NIH, available at http://rsb.info.nih.gov/nih-image/) (Schneider *et al.*, 2012). Particles from frozen conditioned explant media were also collected by centrifugation onto 3-aminopropyltriethoxysilane (APES) coated slides using Shandon Cytofunnel EZ singles with CytoSpin 4 Cytocentrifuge (Thermo Scientific, Basingstoke, UK). The particles were stained with haematoxylin and eosin and imaged (n=3). A threshold of 80µm^2 was employed as this was estimated to be the largest size for red blood cells and single trophoblast cells and <0.2% of SNAs in fresh tissue were smaller than 80µm^2.

Histological examination

Fixed explants were wax embedded and 5µm sections were mounted onto APES coated slides. Cells were fixed by a 20min exposure to ice-cold methanol.

Quantification of SNA number and size

Sections were stained with haematoxylin and eosin to assess SNA number and size. SNAs were defined as clusters of 10 or more nuclei protruding slightly from the villus edge, from either one villus or linking two villi (Cantle *et al.*, 1987). 10 fields of view were imaged and SNAs were counted and

their area measured. Images were analysed using an Olympus BX41 microscope with ImageProPlus 7.0 software (Media Cybernetics, Rockville, MD, USA).

Immunohistochemistry

Endogenous peroxidase activity was quenched using 3% aqueous hydrogen peroxide and non-specific interactions blocked with 10% animal serum. Sections were incubated with 1.1µg/ml mouse monoclonal M30 Cytodeath antibody (Roche), 0.16µg/ml mouse monoclonal Ki67 antibody (Dako MIB-1 clone) or non-specific mouse IgG negative control (1.1µg/ml or 0.16µg/ml as appropriate). Biotinylated goat anti-mouse (Dako; 1:200) and avidin-peroxidase (5µg/ml in 0.125M TBS plus 0.347M NaCl (Jones *et al.*, 1987) were applied and a 3,3-diaminobenzidine treatment was performed to visualise staining. Nuclei were counterstained with Harris' haematoxylin. 10 fields of view were imaged as above and analysed for positive trophoblast nuclei as a percentage of total placental nuclei. Only Ki67 positive cytotrophoblasts were counted as assessed by proximity to the syncytiotrophoblast; other positive nuclei were not included. M30-neoepitope staining was measured in all positive areas as a total of whole explant area.

Immunofluorescence

Immunofluorescence was performed on sections of explant tissue as previously described (Coleman *et al.*, 2013). Briefly, mouse monoclonal anti-β actin AC-74 (Sigma, 1.25µg/ml), anti-γ actin 2-2.1.14.17 (Sigma, 4µg/ml), anti-α tubulin DM1A (Abcam, Cambridge, UK, 1µg/ml), anti-β tubulin (Sigma SAP.4G5 , 0.46µg/ml), anti-cytokeratin 7 (Dako, Glostrup, Denmark, clone OV/TL 12/30, 4.6µg/ml) or corresponding concentrations of non-immune isotype matched mouse IgG were incubated on sections followed by incubation with rabbit anti-mouse FITC (Dako, Glostrup, Denmark, 1:200) and mounted with Vectashield with DAPI or PI to counterstain nuclei (Vector, Burlingame, CA, USA). A Zeiss AxioObserver inverted microscope (Carl Zeiss, Oberkochen, Germany) was used to visualise staining and AxioVision Rel. 4.8 was used to analyse images.

For cell immunofluorescence, a 1% bovine serum albumin (BSA) block was used. Primary antibodies were 1.25µg/ml mouse anti-E-cadherin 610181 (BD Bioscience, San Jose, CA, USA), 5µg/ml rabbit anti-E-cadherin 40772 (Abcam, Cambridge, UK), 2µg/ml mouse anti-α tubulin 7291 (Abcam, Cambridge, UK) or 4.4µg/ml β actin A2228 (Sigma) and secondary antibodies, used at 10µg/ml, were

Alexa Fluor anti-mouse 488, A11029; Alexa Fluor anti-rabbit 488, A11034; or Alexa Fluor anti-mouse 546, A11003, (all Invitrogen, Life Technologies, Grand Island, NY, USA). After staining nuclei with 5μM DRAQ5 (Biostatus Limited, Leicestershire, UK) and mounting using Fluoro-Gel (Electron Microscopy Sciences, Hatfield, PA, USA), images were acquired using a Nikon ECLIPSE E800 (Nikon, Melville, NY) or Olympus FV-500 microscope system equipped with a 60X oil-immersion lens, confocal laser scanning head and three lasers with emissions of 488nm, 546nm, and 633nm. For each cell preparation, 12 fields of view were selected randomly and captured images were analysed using Image J 1.45s (NIH, available at http://rsb.info.nih.gov/nih-image/).

Measurement of inter-nuclear distance

In syncytiotrophoblast, our analyses of inter-nuclear distance were restricted to "large syncytia" (those with 6 or more nuclei) based on previous work which found many syncytia in cultured trophoblasts contain three to five nuclei, with syncytia with 6 or more nuclei representing ~30% of the total (Frendo *et al.*, 2003). We chose these large syncytia for analysis, as they provide more area with a greater ability to detect non-random nuclear localization. Nuclear positioning was quantified only in trophoblasts and syncytia with clearly defined E-cadherin staining that allowed us to clearly identify the cell boundaries. Measurements for cytotrophoblasts were taken from unfused cells with at least one border, estimated as at least half the cell membrane outline, in contact with other unfused cytotrophoblasts, as determined by E-cadherin staining. These criteria were chosen for cytotrophoblast measurements in order to make comparisons with syncytialised nuclei, which lie next to each other. Inter-nuclear distance was determined by measuring the distance between the edge of a nucleus and the edge of its nearest neighbouring nucleus. The designation of SNCs used was based on the results in figure 3D, with a cluster defined as at least six nuclei all with nearest neighbour inter-nuclear distances of ≤3μm; nuclei not meeting this definition were identified as not residing in a cluster. Cells in culture with a highly condensed nuclear morphology are likely to have undergone apoptosis and be non-viable (Longtine *et al.*, 2012b) and were excluded from analysis.

Measurement of cytoplasmic area per nucleus

Cytoplasmic area per nucleus was determined by measuring the cytoplasmic area of adjacent cytotrophoblasts or “large syncytia” using Image J 1.45s (NIH, available at http://rsb.info.nih.gov/nih-

image/) to outline the E-cadherin defined cell borders and dividing that area by the number of nuclei counted in that group of cytotrophoblasts or that syncytium.

Time-lapse microscopy

Time-lapse microscopy was performed on an inverted Nikon TE2000-U microscope. Cells were incubated in a humidified chamber at 37.0°C with 5% CO_2 and 20% O_2 and phase contrast images were recorded every 5 or 10min, typically for 18h, as noted in the figure legends. Videos were generated using Image J 1.45s (NIH, available at http://rsb.info.nih.gov/nih-image/) (Schneider *et al.*, 2012) and annotated in Blender 2.49 (Blender Foundation, Amsterdam, Netherlands).

Statistical analysis

Statistical significance was assessed using Graphpad Prism (Version 5.03, La Jolla, CA). Data were analysed using Kruskal-Wallis test with Dunn's post-hoc test or, when comparing two data sets, using two-way ANOVA. P values ≤0.05 were deemed significant.

In silico model

We modelled the movement of the nuclei as a set of interacting Brownian motions in a two dimensional cross-section of the syncytiotrophoblast layer. Within this two dimensional approximation we were able to include the important features which we hypothesise to play a major role in the formation of large clusters of nuclei within the syncytium. On a long timescale, the nuclei diffuse within the syncytium. The contact forces between cell membranes and the nuclei (and adhesive forces for internuclear interactions) are modelled using a potential which models the forces that each nucleus is subjected to as time evolves. If the radius (R) of a nucleus overlaps with that of another, or with the cell membrane, a large repulsive force is exerted. If the perimeters of two nuclei are within a distance $R<<1$ of each other, then there is a smaller adhesive force which tends to keep the nuclei close to one another.

To include random variation in the thickness of the syncytium, the upper boundary was produced using a polynomial interpolation of a subsampled Ornstein-Uhlenbeck process, leading to a smooth mean zero function (Uhlenbeck and Ornstein, 1930). An Ornstein-Uhlenbeck process has a Gaussian

stationary distribution, and we picked the standard deviation such that the variation is less than 0.75 nuclear diameters with 99.7% confidence. The amplitude of this variation is altered in one set of experiments, where the variation is multiplied by the parameter A. The mean thickness of the cell layer was chosen to be 1.5 nuclear diameters, the parameter which we used to scale the space. The lower boundary was kept as a straight line for simplicity. The length of the domain was chosen to be 250 nuclear diameters, so that using rough estimates of nuclear density at term (29.4% of the volume (Mayhew *et al.*, 1999)), there would be 140 nuclei in the modelled syncytial area. This length is sufficiently long that boundary effects on the result due to this truncation would be minimal.

The contact forces (repulsion and adhesion) between each pair of nuclei were modelled through a potential function V. If the distance between the centres of two nuclei is less than 1 nuclear diameter, then they are overlapping, and the potential function exerts a strong repulsive force. If the two nuclear centres are within a distance x of each other, where $1 < x < 1+R$, and $R = 0.05$ (units are nuclear diameters), then they are assumed to be “stuck together", and a smaller force is exerted on the two nuclei towards each other. The size of this force is determined by a “stickiness", or adhesive, parameter S. If the centres of the two nuclei are further than 1+R away from each other, than it is assumed that there is no interaction between them. Supplementary figure 1 shows the potential function that was used as default within the model and supplementary table 2 lists the parameters from the equation with the values they hold.

As well these forces, each nucleus is also subject to a slow scale diffusion in two dimensions, with diffusion constant D. There is an additional parameter for preferential sites of fusion which is σ, the units of which are in nuclear lengths. The distribution of the fusion sites in this experiment is given by a normal distribution with mean L/2 and variance σ2.

Using this model we investigated factors that could cause nuclei to form SNAs. For the in silico model any clustering of nuclei was measured so ≥2 nuclei adhered to one another was considered a cluster. We explored four different scenarios to give insight into what causes changes in the cluster size and distribution: i) the adhesion of nuclei in internuclear interactions, ii) the rate of diffusion of the nuclei within the syncytium, iii) preferential sites for the fusing of cytotrophoblast nuclei into the syncytium,

and iv) changing/narrowing the width of the cell during the pregnancy. Since the model is stochastic, there is random variation in the results, with each run of the model producing a different configuration of clusters. Therefore, to see the effect on the cluster size distribution, each scenario was repeated 500 times. A scenario is a particular set of values of the parameters. Mostly only one parameter was varied each time, but as diffusion of the nuclei has a negative correlation, and nuclear adhesion a positive correlation on clustering, it was necessary to change both of these values in one experiment (model ii) to keep the adhesiveness at the overall same value, whilst exploring the effect of increased diffusion. At the end point, any two nuclei were considered to be “connected" if they were within a distance 1 + R of each other, i.e. within the radius of interaction. A matrix is formed, each entry of which tells us whether or not each pair of nuclei is connected. From this, using an implementation of Tarjan's algorithm (Tarjan, 1972), all of the clusters were identified.

Results

Before examining SNA dynamics in the placental explant model, we characterised nuclear distribution over time and in response to altered oxygenation to determine optimal conditions for extended explant culture. At 20% O_2, hCG was continuously released, with peak levels between d4 and d8. At 6% O_2, release of hCG occurred on d1 after which lower, baseline levels of hCG were observed (figure 1A). The pattern of hPL release in cultured explants was similar at both 6% and 20% O_2, with a rise at d2, followed by consistent, low secretion for the remaining 16d of culture (figure 1B). There was no significant increase in LDH in the conditioned culture medium at either oxygen concentration, indicating no increase in necrotic cell death (figure 1C). Cytotrophoblasts remaining in-cycle, as assayed by Ki67 staining, were reduced compared to fresh tissue, but the level was maintained throughout culture (figure 1D, F). Cleaved cytokeratin 18 staining increased from very low levels (<0.5%) in fresh tissue to approximately 2% of explant area by d16 of culture in 20% O_2 (figure 1E, G), whereas at 6% O_2, this marker only reached approximately 1% of explant area and while there was a significant increase in staining between fresh tissue and d12, the statistical significance was lost at d16.

We next combined histological examination of nuclear distribution with time at various oxygen levels, with cytological evaluation of shed material. When explants were assessed every 4d up to 16d, no

significant change in SNA density or size was observed. There were no differences in these parameters between the 6% and 20% O_2 conditions (figure 2A and 2B). In fresh tissue, the range of SNA sizes was 80-900μm^2 with 4 exceptions, and over 80% of SNAs were within 80–375μm^2 (figure 2C). Shed material included particles ranging from single cells to pieces of villous tissue and detached syncytiotrophoblast that may contain SNAs (exemplified in figure 2D-F). The shed particles size distribution overlapped with the range observed in SNAs from tissue sections but extended to some much larger particles (approximately 3 times the size of the largest SNAs) and included some villous fragments already known to detach in the explant model (figure 2G). Examples of images taken highlight many single cells, particles that could be SNAs, and one particle that has a villous morphology (figure 2H). There was no significant change in particles shed per mg of explant protein over time (figure 2I; Kruskal-Wallis) with a range of 11–636 particles per 48h per mg explant protein.

Histological analysis of the explants revealed some degree of syncytiotrophoblast shedding from d4, with regrowth of the syncytiotrophoblast noticeable from d8, as previously described (Siman *et al.*, 2001). Newly differentiated nuclei were most obviously seen on d8 and d12 and while they were often adjacent to one another, the nuclei present seemed less numerous and the regrown syncytiotrophoblast was not seen to host SNAs. In placental explants, SNAs were associated with intermediate filament proteins consistently throughout the culture period; in particular, strong cytokeratin 7 immunoreactivity surrounded SNAs in fresh tissue up to d8 (supplementary figure 2). Tubulin staining was found in close proximity to SNAs in fresh tissue up to d8 but there was limited staining on d12 and d16. β-actin was easily observed in fresh tissue, but was harder to identify in the syncytiotrophoblast after that time point, though staining was visible within fibrin deposits (supplementary figure 3).

In primary trophoblast culture, cells were plated as mononucleate cytotrophoblasts and progressively fused, ultimately resulting in most nuclei being within syncytia (cells with 2 or more nuclei/plasma membrane boundary). Groups of associated nuclei, similar to SNAs, were apparent after 2d of culture. Here, we refer to these as "syncytial nuclear clusters" (SNCs) (figure 3A). The proportion of nuclei in “large syncytia” (>6 nuclei) (~40%) showed no significant change over 2-6d in culture. Similarly, the proportion of nuclei in these “large syncytia” that had gathered into SNCs showed no

significant change over the culture period (figure 3B). Trophoblasts and syncytia that had undergone apoptosis as indicated by condensed nuclei visible in phase contrast microscopy (Longtine *et al.*, 2012b) were visible in culture from day 3. Qualitatively these apoptotic regions were sparse and covered small areas at day 3, becoming increasingly common by days 5-6 (supplementary figure 4). For subsequent analyses, measurements were only taken from trophoblasts without condensed nuclei. The median inter-nuclear distance was significantly smaller in syncytia than in unfused adjacent cytotrophoblasts: 0.81μm vs. 4.99μm ($p>0.001$), but neither value changed significantly during culture (figure 3C). While internuclear distance showed little change, there was a significantly higher cytoplasmic area per nucleus in syncytia (figure 3D) after 4d ($p\geq0.05$) and 6d of culture ($p\geq0.001$) in comparison to that seen in unfused cytotrophoblast cells, which retained a similar cytoplasmic area per nucleus throughout the culture period (figure 3E).

To investigate whether cytoskeletal components were involved in SNC formation and maintenance, microfilaments and microtubules were disrupted in primary cell culture by exposure to cytochalasin D or nocodazole, respectively. Based on immunofluorescence images, E-cadherin continued to identify cell boundaries after 2h cytochalasin D and nocodazole treatment, but the treatments disrupted actin and tubulin, respectively (figure 4A and 4B). Cytochalasin D treatment changed filamentous actin to a globular form and nocodazole treatment changed longer organised microtubules, particularly seen around the edges of syncytia, to disrupted shorter fragments. Treatment with cytochalasin or nocodazole for 6h did not significantly diminish the proportion of nuclei in SNCs in syncytiotrophoblast (figure 4C). Likewise, treatment with cytochalasin or nocodazole for 18h before fusion had reached a maximum level at 40-42h of culture had no effect on the percentage of nuclei in “large syncytia” (>6 nuclei) or in SNCs (figure 4D and 4E, respectively). Actin was depolymerised in explants cultured for 24h then treated with cytochalasin D for 20h (supplementary figure 5). Nocodazole depolymerized tubulin in explants and paclitaxel stabilised tubulin in explants over the same time frame (supplementary figure 5). However, there was no significant change in SNA density after treating explants with cytochalasin D (figure 4F), nocodazole (figure 4G) or paclitaxel (figure 4H).

Time-lapse imaging of cultured primary trophoblasts revealed that nuclei in SNCs were remarkably stable in their position within the cell and in their positions relative to one another. Nuclear movement

was only observed with associated movement of the cell membranes, for instance, during the initial spreading of trophoblasts on the tissue culture plate (supplementary video 1). Between d2-4, there was little change in relative nuclear positions (supplementary videos 2, 3). Cytochalasin D and nocodazole affected the ability of the cultured trophoblasts and syncytia to maintain their shape; again cell membrane movement was associated with nuclear movement (supplementary videos 4-6).

A mathematical model was devised as a tool for examining the effects of factors that might affect nuclear distribution, assuming stochastic progression from a baseline. The set variables included: diameter that cytotrophoblast fusion can occur within; tendency of nuclei to remain associated once in proximity to one another; rate of nuclear movement within the syncytial boundary and changes in thickness of the syncytial boundary. To address the impact of these individual factors on formation and size of nuclear clusters (≥2 connected nuclei), the in silico model was run on multiple occasions and this produced well converged statistics. In this model the number of clusters with more than 6 nuclei increased over time, mimicking the in vivo situation. Figure 5 shows a sample of the post-processed results and the analysis. Mean cluster size increased with nuclear adhesiveness (figure 5A). The rate of nuclear movement had a non-linear effect on clustering; initially increasing the rate of movement increased the rate of nuclear collisions and thus the likelihood of adhesion, but as the rate increased further, the nuclei were more likely to become unstuck from one another (figure 5B). When sites of cytotrophoblast fusion were closer to one another (when σ is low) the rate of clustering increased (figure 5C). Varying the thickness of the syncytium produced no effect on clustering (figure 5D). Examples of the visualization produced by the in silico model when there is high or low nuclear clustering are shown (figure 5E).

Discussion

In vivo, SNAs increase in number as pregnancy progresses and are increased in pregnancy complications, most notably preeclampsia. This observation suggests nuclei in the syncytiotrophoblast are not constrained within the cytoplasmic architecture, consequently we hypothesised that SNA formation is an active process involving cytoskeletal-driven nuclear motility. However, this hypothesis was not borne out; we have demonstrated that there is comparatively little SNA development in term villous explant culture and little nuclear movement within multinuclear

syncytia in primary trophoblast culture. Furthermore, neither the stability nor formation of SNAs is affected by pharmacological disruption of the microfilament or microtubular cytoskeleton. The in silico model suggests that formation of nuclear clusters may be promoted by preferential fusion of cytotrophoblast in the region of SNAs or by characteristics of the nuclei (e.g. adhesiveness). This observational data suggest that nuclei in the syncytiotrophoblast are not highly mobile and that it is necessary to seek other mechanisms to explain in vivo SNA formation, and why they are increased in pregnancy pathologies.

Both cell and explant models were cultured for extended periods as SNAs are thought to be markers of more mature syncytiotrophoblast, appearing towards term and more often in prolonged pregnancies (Jones and Fox, 1978; Al-Allaf *et al.*, 2008). Explants were employed as they maintain the full three-dimensional villous structure and have been used previously to investigate the development of SNAs (Heazell *et al.*, 2008b). However, data obtained in extended static explant culture are necessarily limited and must be treated with caution; the absence of normal endocrine function clearly indicates that syncytial properties are impaired. During culture the basic structure of the villous tissue remained intact, with minimally increased LDH release and a similar rate of proliferation to that seen in vivo. Some evidence suggested that this extended culture exceeds optimum viability of explants and responsiveness after 8d, including reduced hCG release, loss of E-cadherin and increased M30 staining. However, the persistence of Ki67 staining to 16d indicates potential for fusion of new cytotrophoblasts and formation of new SNAs throughout the culture period. Consequently, the lack of change in SNAs throughout this culture period, which also includes the usual timeframe of culture at the beginning, suggests that the lack of SNA formation reflects syncytiotrophoblast behaviour. This evidence opposes judgements that explant vitality decline, due to prolonged culture, is the sole cause for the lack of SNA formation. Both explant and cell models showed signs of apoptosis with increased M30 staining in explants and visible apoptotic cells in primary trophoblast culture. Apoptosis has been linked to SNA formation: however, the relationship between terminal differentiation and apoptosis in the syncytiotrophoblast has not been conclusively established, even if some of the same machinery may be used (Coleman *et al.*, 2013; Rote *et al.*, 2010). The lack of association between increased M30 staining, a terminal product of apoptosis, and

458 SNA formation in placental explants here and elsewhere (Longtine *et al.*, 2012a) provides further
459 evidence that SNA formation is not coincident with apoptosis.
460
461 The explant model allows at least a rough evaluation of the potential of SNAs to remain stable, to alter
462 in number or form, or to be lost from the tissue, over a period of over 2 weeks (admittedly in the
463 absence of maternal circulatory flow). The observations show there was no evidence of change in
464 explant SNA size or number during a period of over 2 weeks (figure 2A &B). In addition to some non-
465 specific delamination (and replacement) of syncytial strips, as previously reported (Siman *et al.*,
466 2001), particles in the size range of SNAs were shed, which may mimic release from the placenta
467 during throughout pregnancy as trophoblast deportation (Askelund and Chamley, 2011). In tissue, we
468 estimate that there were approximately 3800 SNAs/mg protein and the median number of particles of
469 comparable size to SNAs shed in 48h was 77 particles/mg protein, equating to approximately 2% of
470 the total SNAs present (Coleman *et al.*, 2013). Critically, the rate of release did not change over the
471 culture period, suggesting little requirement for replacement during culture. Potentially, particles shed
472 by the placenta into maternal circulation could arise more commonly from syncytial sprouts than
473 SNAs, especially in early pregnancy, though opinion on this is varied in the scientific community
474 (Chamley *et al.*, 2014). Thus, the modest loss and generation of SNAs that we observed in explants
475 could mirror in vivo events. The data suggest that the generation of SNAs in third trimester placenta is
476 not primarily a developmental device for the disposal of unwanted (and possibly effete) nuclei. It may
477 be that mechanisms other than the release of SNAs, such as loss of syncytial fragments, account for
478 the large quantities of fetal DNA found in maternal circulation (Bianchi, 2004).
479
480 In primary trophoblast culture, syncytial nuclei were, on average, closer together than nuclei found in
481 adjacent cytotrophoblasts. It is possible that the lower inter-nuclear distances and higher cytoplasmic
482 area per nucleus in syncytiotrophoblast compared to precursor cytotrophoblasts may give the
483 appearance of forming nuclear clusters, rather than an active process by which nuclei are
484 aggregated. The changes in cytoplasmic area may be caused by cytoplasmic redistribution (thinning
485 and spreading) after cytotrophoblast fusion with syncytiotrophoblast but could also be caused by an
486 increase in cell volume. Notably, nuclei within syncytia in cultured trophoblasts moved very little, and
487 the newly formed SNCs (and also SNAs in explant culture), were not vulnerable to separation after

inhibitor-based disruption and depolymerisation of the microfilament and the microtubule cytoskeletons.

In explants, the lack of movement could be due to cytochalasin D and nocodazole exerting effects only while present in culture medium, with normal actin and tubulin structure returning after their removal (Friederich *et al.*, 1993; Zieve *et al.*, 1980; Rhee *et al.*, 2007), but in primary cytotrophoblasts there was no treatment-free interval prior to fixation. If SNAs were actively maintained by actin or tubulin it was expected that treatment with cytoskeletal disruptors would cause a reduction in SNA size or number. So, despite the pulsatile nature of the treatment in explants, as there was no change in SNA numbers after treatment, these data are most consistent with actin and tubulin function being not required to maintain SNAs. It is also possible that the surrounding cisternae of endoplasmic reticulum may exert a restraining influence. Furthermore, given the low levels of cytotrophoblast proliferation in term placental tissue, it is unlikely that compensatory formation of SNAs could have occurred.

The observations that cytoskeletal inhibitors had no significant effect on SNA or SNC counts suggest there may not be an active nuclear transport mechanism that uses cytoskeletal components present in the syncytiotrophoblast. The lack of nuclear movement despite changes in cytoplasmic area, which would be expected to increase inter-nuclear distance, may indicate that nuclear positioning is mainly determined by the point of initial fusion and then maintained throughout culture. In primary trophoblast, clustering could increase over time as nuclei initially fuse to a similar position, group together and take up a lesser proportion of cytoplasmic area. Meanwhile, expansion of the cytoplasmic area of the syncytium may occur as protein biosynthesis produces secretory machinery, other organelles, membranes and cellular components.

Selected fusion of cytotrophoblasts into the syncytiotrophoblast may be important for SNA formation. Previously, cytoskeletal disruptors have been shown to negatively affect cytotrophoblast fusion if added at 6h (Douglas and King, 1993) and this may have had an effect on the early incubation and explant studies. As primary cytotrophoblasts predominantly fuse between 24-48h (Kliman *et al.*, 1986), 72h was selected to obtain mature syncytia with SNCs. It is possible that the earlier treatment

518 at 40-42h could have interrupted fusion events (Richard *et al.*, 2009). However, the time between 6-
519 24h may have allowed fusion pores to form, so that the cytoskeletal disruption which happened later
520 had a minimal effect on fusion (Richard *et al.*, 2009). The lack of an effect of cytoskeletal inhibitors on
521 cytotrophoblast fusion indicates that most fusion events had already occurred by 40-42h. In explants it
522 is possible that proliferation of cytotrophoblast and incorporation into the overlying syncytium was
523 inhibited by addition of disruptors at 24h.
524
525 Exploration of SNC formation using the in silico model, informed by experimental data, identified
526 factors that could be responsible for the formation and maintenance of SNAs/SNCs. These may be
527 grouped into two types of effect: an increased likelihood of collisions between nuclei and an increased
528 likelihood that two adjacent nuclei will become stably associated. For example, increasing nuclear
529 proximity and adherence promotes cluster formation. In contrast, the correlation between the diffusion
530 rate (D) of the nuclei, and the average cluster size is less clear. As the diffusion rate of the nuclei
531 increases from zero, more collisions occur, resulting in more nuclei forming clusters. However, as this
532 diffusion rate continues to increase, the nuclei do not stay together, and average cluster size
533 decreases. Lastly, if sites where cytotrophoblasts fuse into the syncytium are non-uniformly
534 distributed then the distribution of nuclei is less uniform, with more packed together in certain regions,
535 thereby resulting in more collisions and a higher average cluster size. Our numerical surveys looked
536 at a range of causes of both of these effects, which had differing influence on the cluster size
537 distribution. This analysis shows that clustering requires either nuclear diffusion or preferential sites
538 for the introduction of new nuclei into the syncytium, or both. Once regular collisions between nuclei
539 occur, the adherence of the nuclei then plays a significant role in the cluster size distribution.
540
541 Whatever the mechanism by which they approach one another, we have two hypotheses for how
542 nuclei stay together in clusters. First, it is possible that intermediate filaments stabilise nuclear
543 clusters, supported by the observation that grouped nuclei are enmeshed in cytokeratin filament
544 arrays (Jones and Fox, 1977; Beham *et al.*, 1988; Bradbury and Ockleford, 1990; Coleman *et al.*,
545 2013). This leads to further speculation that nuclear proximity can activate intermediate filament
546 assembly, possibly relying on association between elements of the outer nuclear envelope and
547 components of the cytoskeleton. Second, proteins on or in the outer nuclear envelope may be able to

548 bind to similarly localized proteins on adjacent intervening cytoplasmic membranes, making nuclei
549 adherent. While evidence for nuclear adhesion in placenta is limited, proteins on the nuclear envelope
550 or endoplasmic reticulum that are involved with nuclear stabilisation, including elements of the linker
551 of nucleoskeleton and cytoskeleton complex (LINC), SUN and KASH proteins (Starr, 2007), are
552 transcribed in the placenta (supplementary table 3) (http://www.ncbi.nlm.nih.gov/unigene,
553 05/10/2015). In yeast and *Caenorhabditis elegans* the LINC complex participates in transcription,
554 DNA repair and signalling pathways which may be disrupted in SNAs (Kim *et al.*, 2015). Thus the role
555 of LINC complex merits further investigation in human placenta.
556
557 Another possibility is that the position of cytotrophoblast fusion relative to overlying syncytioplasm
558 may contribute to SNA formation, as fusion sites proximal to syncytial nuclei would effectively create
559 groups of nuclei without the need for nuclear motility. Such a mechanism requires either concentrated
560 areas for cytotrophoblast replication or cytotrophoblast motility in tissue, this has not been
561 demonstrated conclusively in vitro but remains a possibility. In this context, it is noteworthy that
562 extravillous trophoblasts of the human placenta are dramatically migratory, deeply invading maternal
563 tissues (McKinnon *et al.*, 2013). It will be of interest to determine if villous cytotrophoblasts are able to
564 move within villous tissue - such movement may be condition dependent, and require the presence of
565 hormones and other factors that are not typically present in in vitro culture. This hypothesis deviates
566 fundamentally from the earlier suggestion that nuclei are collected into aggregates by an active
567 process, specifically towards the end of their lifespan in syncytium (Huppertz *et al.*, 2006). The latter
568 hypothesis has been criticised on the basis that transcriptional activity can be found in nuclei within
569 SNAs, that is, they are not simply repositories of inactive, pyknotic nuclei destined for apoptosis. This
570 hypothesis also has relevance for preeclampsia, where an increased rate of cytotrophoblast fusion
571 would provide more nuclei that could contribute to SNAs (Arnholdt *et al.*, 1991; Huppertz *et al.*, 2002;
572 Heazell *et al.*, 2006). This formation of SNAs could be further magnified by oxidative stress, as nuclei
573 within syncytial knots, in particular show increased levels of oxidative damage (Chaddha *et al.*, 2004;
574 Crocker *et al.*, 2004; Germain *et al.*, 2007; Fogarty *et al.*, 2013). Overall, these hypotheses suggest a
575 mechanism for SNA formation within normal placental development which can be accelerated in
576 aging and pregnancy complications.
577

Further experiments are required to further explore the events leading to SNA formation. To study cytotrophoblast fusion and progression into SNAs, floating term placental explants could be denuded of the original syncytiotrophoblast with trypsin and the formation of new SNAs quantified during and after formation of new syncytium. To address the hypothesis that there are preferential sites for fusion, the locations of the newly merged nuclei could be mapped. If newly merged nuclei tend to stay close to each other, this would provide a strong indication that there are preferential fusion sites. If a denuded explant model produced enough syncytiotrophoblast to contain SNAs it may then provide a starting point for further experiments with inhibitors or BrdU pulse-chase experiments, which could reveal if newly merged nuclei join with existing SNAs they tend to stay with nuclei of the same metabolic “age”. Further work could also be done into possible interactions between nuclei using explant and cell models. A pull-down assay against nuclear lamins could be performed on syncytiotrophoblast and primary cytotrophoblasts encouraged to fuse in culture. After the pull-down, the contents could be fixed onto slides using a cytospin and imaged to see if nuclei are always individual or if SNAs are pulled down, indicative of connections between nuclei. Then inhibitors or proteases could be added to cultures to see what disrupts nuclear clustering.

In conclusion, nuclei in syncytiotrophoblast appear surprisingly static. SNAs in tissue, and SNCs that form in culture are closely enveloped by cytokeratin filaments and neither their formation nor their stability are altered by treatment with actin or tubulin disruptors. Mechanisms other than active nuclear movement within the syncytiotrophoblast cytoplasm are major contributors to SNA formation. Furthermore, our results provide little evidence in support of the hypothesis that SNA "turnover" occurs via specific shedding of SNAs into the maternal circulation. These findings have implications for our understanding of excessive SNA formation in pregnancy disorders. Together, our work strongly suggests that further evaluation of mechanisms of SNA formation and of their significance in complicated pregnancies is warranted.

Funding

This work was funded by Tommy's and a Medical Research Council PhD Studentship.

For work performed at the University of Manchester support is appreciated from an Action Research Endowment Fund and the Manchester Biomedical Research Centre.

For work performed at Washington University School of Medicine supporting grants were received from Boehringer Ingelheim Fonds for travel and the NIH to D. M. Nelson (RO1 HD 29190).

Acknowledgements

For work performed at the University of Manchester, we would like to thank the University of Manchester Bioimaging Centre for use of their facilities and technical assistance with special thanks to Peter March and Steve Marsden. Microscopes used in this study were purchased with grants from BBSRC, Wellcome and the University of Manchester Strategic Fund. We also appreciate the help of Dr. Karen Forbes, Dr. Susan Greenwood and Dr. Mark Wareing.

For work performed at Washington University School of Medicine, we would like to thank The Foundation for Barnes-Jewish Hospital, St. Louis, MO, U.S.A. We appreciate the technical assistance of Dr. Baosheng Chen and Dennis Oakley from the Bakewell Neuroimaging Laboratory.

Final thanks go to Ian Calvert for his assistance with video annotation.

Declaration of Interests

The authors declare no conflict of interests that could be perceived as prejudicing the impartiality of the research reported.

References

Al-Allaf L, Jarjees M and Al-Nuaimy W (2008) Histological changes of human placenta in prolonged pregnancy. *JBMS Journal of the Bahrain Medical Society* **20** 60–67.

Aplin JD (2010) Developmental cell biology of human villous trophoblast: current research problems. *The International Journal of Developmental Biology* **54** 323–329.

Arnholdt H, Meisel F, Fandrey K and Löhrs U (1991) Proliferation of villous trophoblast of the human placenta in normal and abnormal pregnancies. *Virchows Archiv. B, Cell Pathology Including Molecular Pathology* **60** 365–372.

Askelund K and Chamley L (2011) Trophoblast deportation part I: review of the evidence demonstrating trophoblast shedding and deportation during human pregnancy. *Placenta* **32** 716–723.

Audette MC, Greenwood SL, Sibley CP, Jones CJP, Challis JRG, Matthews SG and Jones RL (2010) Dexamethasone stimulates placental system A transport and trophoblast differentiation in term villous explants. *Placenta* **31** 97–105.

Beham A, Denk H and Desoye G (1988) The distribution of intermediate filament proteins, actin and desmoplakins in human placental tissue as revealed by polyclonal and monoclonal antibodies. *Placenta* **9** 479–492.

Bianchi DW (2004) Circulating fetal DNA: its origin and diagnostic potential-a review. *Placenta* **25** Suppl A S93–S101.

Boyd JD and Hamilton WJ (1967) Development and structure of the human placenta from the end of the 3rd month of gestation. *The Journal of Obstetrics and Gynaecology of the British Commonwealth* **74** 161–226.

Boyd JD and Hamilton WJ (1970) The Human Placenta. *Heffer.*

Bradbury FM and Ockleford CD (1990) A confocal and conventional epifluorescence microscope study of the intermediate filaments in chorionic villi. *Journal of Anatomy* **169** 173–187.

Burton GJ and Jones CJP (2009) Syncytial knots, sprouts, apoptosis, and trophoblast deportation from the human placenta. *Taiwanese Journal of Obstetrics and Gynecology* **48** 28–37.

Calvert SJ, Jones CJP, Sibley CP, Aplin JD and Heazell AEP (2013) Analysis of syncytial nuclear aggregates in preeclampsia shows increased sectioning artefacts and decreased inter-villous bridges compared to healthy placentas. *Placenta* **34** 1251–1254.

Cantle SJ, Kaufmann P, Luckhardt M and Schweikhart G (1987) Interpretation of syncytial sprouts and bridges in the human placenta. *Placenta* **8** 221–234.

Carvalho L, Stuhmer J, Bois JS, Kalaidzidis Y, Lecaudey V and Heisenberg CP (2009) Control of convergent yolk syncytial layer nuclear movement in zebrafish. *Development* **136** 1305–1315.

Chaddha V, Viero S, Huppertz B and Kingdom J (2004) Developmental biology of the placenta and the origins of placental insufficiency. *Seminars in Fetal and Neonatal Medicine* **9** 357–369.

Chamley LW, Holland OJ, Chen Q, Viall CA, Stone PR and Abumaree M (2014) Review: Where is the maternofetal interface? *Placenta* **35** S74–S80.

Chen B, Nelson DM and Sadovsky Y (2006) N-myc down-regulated gene 1 modulates the response of term human trophoblasts to hypoxic injury. *The Journal of Biological Chemistry* **281** 2764–2772.

Chen B, Longtine MS and Nelson DM (2013) Pericellular oxygen concentration of cultured primary human trophoblasts. *Placenta* **34** 106–109.

Coleman SJ, Gerza L, Jones CJP, Sibley CP, Aplin JD and Heazell AEP (2013) Syncytial nuclear aggregates in normal placenta show increased nuclear condensation, but apoptosis and cytoskeletal redistribution are uncommon. *Placenta* **34** 449–455.

Corrêa RRM, Gilio DB, Cavellani CL, Paschoini MC, Oliveira FA, Peres LC, Reis MA, Teixeira VPA and Castro ECC (2008) Placental morphometrical and histopathology changes in the different clinical presentations of hypertensive syndromes in pregnancy. *Archives of Gynecology and Obstetrics* **277** 201–206.

Crocker IP, Tansinda DM and Baker PN (2004) Altered cell kinetics in cultured placental villous explants in pregnancies complicated by pre-eclampsia and intrauterine growth restriction. *The Journal of Pathology* **204** 11–18.

Douglas GC and King BF (1993) Colchicine inhibits human trophoblast differentiation in vitro. *Placenta* **14** 187–201.

Fogarty NME, Ferguson-Smith AC and Burton GJ (2013) Syncytial knots (Tenney-Parker changes) in the human placenta: evidence of loss of transcriptional activity and oxidative damage. *The American Journal of Pathology* **183** 144–152.

Frendo JL, Cronier L, Bertin G, Guibourdenche J, Vidaud M, Evain-Brion D and Malassine A (2003) Involvement of connexin 43 in human trophoblast cell fusion and differentiation. *Journal of Cell Science* **116** 3413–3421.

687 **Friederich E, Kreis TE and Louvard D** (1993) Villin-induced growth of microvilli is reversibly inhibited
688 by cytochalasin D. *Journal of Cell Science* **105** 765–775.
689 **Frock RL, Kudlow BA, Evans AM, Jameson SA, Hauschka SD and Kennedy BK** (2006) Lamin
690 A/C and emerin are critical for skeletal muscle satellite cell differentiation. *Genes & Development* **20**
691 486–500.
692 **Garcia-Lloret MI, Yui J, Winkler-Lowen B and Guilbert LJ** (1996) Epidermal growth factor inhibits
693 cytokine-induced apoptosis of primary human trophoblasts. *Journal of Cellular Physiology* **167** 324–
694 332.
695 **Germain SJ, Sacks GP, Soorana SR, Sargent IL and Redman CW** (2007) Systemic inflammatory
696 priming in normal pregnancy and preeclampsia: the role of circulating syncytiotrophoblast
697 microparticles. *The Journal of Immunology* **178** 5949–5956.
698 **Goswami D, Tannetta DS, Magee LA, Fuchisawa A, Redman CWG, Sargent IL and von**
699 **Dadelszen P** (2006) Excess syncytiotrophoblast microparticle shedding is a feature of early-onset
700 pre-eclampsia, but not normotensive intrauterine growth restriction. *Placenta* **27** 56–61.
701 **Hahn S, Huppertz B and Holzgreve W** (2005) Fetal cells and cell free fetal nucleic acids in maternal
702 blood: new tools to study abnormal placentation? *Placenta* **26** 515–526.
703 **Heazell A, Harris L, Forbes K and Crocker I** (2006) Placental cell turnover in health and disease.
704 *Reviews in Gynaecological and Perinatal Practice* **6** 80–86.
705 **Heazell AEP, Moll SJ, Jones CJP, Baker PN and Crocker IP** (2007) Formation of syncytial knots is
706 increased by hyperoxia, hypoxia and reactive oxygen species. *Placenta* **28** S33–S40.
707 **Heazell AEP, Buttle HR, Baker PN and Crocker IP** (2008a) Altered expression of regulators of
708 caspase activity within trophoblast of normal pregnancies and pregnancies complicated by
709 preeclampsia. *Reproductive Sciences* **15** 1034–1043.
710 **Heazell AEP, Lacey HA, Jones CJP, Huppertz B, Baker PN and Crocker IP** (2008b) Effects of
711 oxygen on cell turnover and expression of regulators of apoptosis in human placental trophoblast.
712 *Placenta* **29** 175–186.
713 **Humphrey RG, Sonnenberg-Hirche C, Smith SD, Hu C, Barton A, Sadovsky Y and Nelson DM**
714 (2008) Epidermal growth factor abrogates hypoxia-induced apoptosis in cultured human trophoblasts
715 through phosphorylation of BAD Serine 112. *Endocrinology* **149** 2131–2137.

716 **Huppertz B, Kaufmann P and Kingdom J** (2002) Trophoblast turnover in health and disease. *Fetal*
717 *and Maternal Medicine Review* **13** 103–118.
718 **Huppertz B, Kingdom J, Caniggia I, Desoye G, Black S, Korr H and Kaufmann P** (2003) Hypoxia
719 favours necrotic versus apoptotic shedding of placental syncytiotrophoblast into the maternal
720 circulation. Placenta 24 181–190.
721 **Huppertz B, Kadyrov M and Kingdom JCP** (2006) Apoptosis and its role in the trophoblast.
722 *American Journal of Obstetrics and Gynecology* **195** 29–39.
723 **Jauniaux E, Watson AL, Hempstock J, Bao YP, Skepper JN and Burton GJ** (2000) Onset of
724 maternal arterial blood flow and placental oxidative stress. A possible factor in human early
725 pregnancy failure. *American Journal of Pathology* **157** 2111–2122.
726 **Johnstone ED, Sibley CP, Lowen B and Guilbert LJ** (2005) Epidermal growth factor stimulation of
727 trophoblast differentiation requires MAPK11/14 (p38 MAP kinase) activation. *Biology of Reproduction*
728 **73** 1282–1288.
729 **Jones CJP and Fox H** (1977) Syncytial knots and intervillous bridges in the human placenta: an
730 ultrastructural study. *Journal of Anatomy* **124** 275–286.
731 **Jones CJP and Fox H** (1978) Ultrastructure of the placenta in prolonged pregnancy. *Journal of*
732 *Pathology* **126** 173-179.
733 **Jones CJP, Mosley SM, Jeffrey IJM and Stoddart RW** (1987) Elimination of the non-specific
734 binding of avidin to tissue sections. *Histochemical Journal* **19** 264–268.
735 **Kim DI, Birendra KC and Roux KJ** (2015) Making the LINC: SUN and KASH protein interactions.
736 *Biological Chemistry* **396** 295–310.
737 **Kliman HJ, Nestler JE, Sermasi E, Sanger JM and Strauss JF** (1986) Purification,
738 Characterization, and in vitro Differentiation of Cytotrophoblasts from Human Term Placentae.
739 *Endocrinology* **118** 1567–1582.
740 **Longtine M, Chen B, Odibo A, Zhong Y and Nelson D** (2012a) Caspase-mediated apoptosis of
741 trophoblasts in term human placental villi is restricted to cytotrophoblasts and absent from the
742 multinucleated syncytiotrophoblast. *Reproduction* **143** 107–121.
743 **Longtine MS, Barton A, Chen B and Nelson DM** (2012b) Live-cell imaging shows apoptosis initiates
744 locally and propagates as a wave throughout syncytiotrophoblasts in primary cultures of human
745 placental villous trophoblasts. *Placenta* **33** 971–976.

Malone CJ, Fixsen WD, Horvitz HR and Han M (1999) UNC-84 localizes to the nuclear envelope and is required for nuclear migration and anchoring during C. elegans development. *Development* **126** 3171–3181.

Mayhew TM (2014) Turnover of human villous trophoblast in normal pregnancy: what do we know and what do we need to know? *Placenta* **35** 229–240.

Mayhew TM, Leach L, McGee R, Ismail WW, Myklebust R and Lammiman MJ (1999) Proliferation, differentiation and apoptosis in villous trophoblast at 13-41 weeks of gestation (including observations on annulate lamellae and nuclear pore complexes). *Placenta* **20** 407–422.

McKinnon T, Chakraborty C, Gleeson LM, Chidiac P and Lala PK (2013) Stimulation of human extravillous trophoblast migration by IGF-II is mediated by IGF type 2 receptor involving inhibitory G Protein(s) and phosphorylation of MAPK. *The Journal of Clinical Endocrinology & Metabolism* **86** 3665–3674.

Metzen E, Wolff M, Fandrey J and Jelkmann W (1995) Pericellular P_{O2} and O_2 consumption in monolayer cell cultures. *Respiration Physiology* **100** 101–106.

Moll SJ, Jones CJP, Crocker IP, Baker PN and Heazell AEP (2007) Epidermal growth factor rescues trophoblast apoptosis induced by reactive oxygen species. *Apoptosis* **12** 1611–1622.

Morrish DW, Bhardwaj D, Dabbagh LK, Marusyk H and Siy O (1987) Epidermal growth factor induces differentiation and secretion of human chorionic gonadotropin and placental lactogen in normal human placenta. *Journal of Clinical Endocrinology & Metabolism* **65** 1282–1290.

Morrish DW, Dakour J, Li H, Xiao J, Miller R, Sherburne R, Berdan RC and Guilbert LJ (1997) In vitro cultured human term cytotrophoblast: A model for normal primary epithelial cells demonstrating a spontaneous differentiation programme that requires EGF for extensive development of syncytium. *Placenta* **18** 577–585.

Pettersen EO, Larsen LH, Ramsing NB and Ebbensen P (2005) Pericellular oxygen depletion during ordinary tissue culturing, measured with oxygen microsensors. *Cell Proliferation* **38** 257–267.

Pringle KG, Kind KL, Sferruzzi-Perri AN, Thompson JG and Roberts CT (2010) Beyond oxygen: complex regulation and activity of hypoxia inducible factors in pregnancy. *Human Reproduction Update* **16** 415–431.

Richard J, Leikina E and Chernomordik L (2009) Cytoskeleton reorganization in influenza hemagglutinin-initiated syncytium formation. *Biochimica et Biophysica Acta* **1788** 450–457.

Rhee S, Jiang H, Ho C-H and Grinnell F (2007) Microtubule function in fibroblast spreading is modulated according to the tension state of cell-matrix interactions. *Proceedings of the National Academy of Sciences of the United States of America* **104** 5425–5430.

Rote NS, Wei B-R, Xu C, Luo L (2010) Caspase 8 and human villous cytotrophoblast differentiation. *Placenta* **31** 89–96.

Schneider CA, Rasband WS and Eliceiri KW (2012) NIH Image to ImageJ: 25 years of image analysis. *Nature Methods* **9** 671–675.

Siman CM, Sibley CP, Jones CJP, Turner MA and Greenwood SL (2001) The functional regeneration of syncytiotrophoblast in cultured explants of term placenta. *American Journal of Physiology- Regulatory, Integrative and Comparative Physiology* **280** R1116–R1122.

Starr DA (2007) Communication between the cytoskeleton and the nuclear envelope to position the nucleus. *Molecular Biosystems* **3** 583–589.

Sullivan M, Galea P and Latif S (2006) What is the appropriate oxygen tension for in vitro culture? *Molecular Human Reproduction* **12** 653.

Tarjan R (1972) Depth-first search and linear graph algorithms. *SIAM Journal on Computing* **1** 146–160.

Tenney B and Parker F (1940) The placenta in toxemia of pregnancy. *American Journal of Obstetrics and Gynecology* **39** 1000–1005.

Tuuli MG, Longtine MS and Nelson DM (2011) Review: oxygen and trophoblast biology–a source of controversy. *Placenta* **32** S109–S118.

Uhlenbeck GE and Ornstein LS (1930) On the theory of the Brownian motion. *Physical Review* **36** 823–841.

Zieve GW, Turnbull D, Mullins JM and McIntosh JR (1980) Production of large numbers of mitotic mammalian cells by use of the reversible microtubule inhibitor Nocodazole. *Experimental Cell Research* **126** 397–405.

Figure Legends

Figure 1 - (A) There was a significant difference in hCG production between the two oxygen concentrations as assessed by two-way ANOVA at days 1 and 4-8. (B) A black (20% O_2 colour) or grey (6% O_2 colour) significance bar at the top relates to a significant difference between hPL production between days 2, 3 or 4 and a later time point assessed by Kruskal-Wallis test. (C) There were no significant differences in LDH release across the culture period. (D) Ki67 staining reduced from day 0 compared to days 4, 8 and 16 at 6% O_2. (E) Apoptosis, assessed by staining for the M30 neoepitope, significantly increased at day 16 in 20% O_2 compared to 6% O_2 (black significance bar at right) (two-way ANOVA). Staining was increased after Day 8 in 20% O_2 (black significance bars at top) and between Days 0 and 12 in 6% O_2 (grey significance bar at top) Kruskal-Wallis test. (F) Representative images of the reduction in Ki67 positive trophoblast across the time frame and (G) M30 neoepitope increased staining with time at 20% O_2. (Scale bars =20µm). *p<0.05, **p<0.01, ***p<0.001 (n=6; median and interquartile range). The key next to graph 1E applies to all graphs on figure 1.

Figure 2 - (A) The density and (B) size of SNAs do not change over the 16 day culture period or in different oxygen tensions when assessed by two-way ANOVA and Kruskal-Wallis test (n=6; median and interquartile range). (C) The size range of SNAs demonstrates the majority are between 150-375µm (n=11; fresh tissue), one point of 1826 was excluded from this graph. Tissue fragments collected from explants-conditioned medium stained with haematoxylin and eosin, (D) individual cells, (E) villous tissue lost from an explant and (F) structure similar to an SNA with several nuclei grouped closely together (Scale bars = 20µm). (G) Most particles analysed had a measurement in the

lower (SNA) size range (n=4). (H) A representative image of DAPI stained particles shed into culture media; approximately 1/10 of the well is shown. Examples of single cells (filled arrows) are shown that were below 80µm; several particles that could be SNAs are indicated by open arrows. One villus fragment is marked by *. Scale bar = 200µm. (I) There was no significant change in number of fragments ≥80µm^2 lost over time into culture medium (n=4; Kruskal-Wallis test).

Figure 3 – (A) Representative image of an SNC in isolated cytotrophoblast cell-culture. (B) There was no change in the percentage of nuclei in large syncytia or in SNC over 6 days of culture. (C) Inter-nuclear distances were smaller in large syncytia compared to cytotrophoblast cells (Median and interquartile range in box plot with whiskers extending between the 1st and 99th percentile; *** $p<0.001$). (D) An example of areas selected for measurements as "adjacent cytotrophoblast cells" and large syncytia are shown in white and red, respectively. (E) Large syncytia had a significantly greater ratio of cytoplasmic area to nuclei than cytotrophoblasts on Days 4 and 6 of culture. Graph shows median and interquartile range assessed by Kruskal-Wallis test; *$p<0.05$, ***$p<0.001$ (n=3).

Figure 4 – Representative images of (A) control cells (red gain 7.60) and cells treated with cytochalasin D (red gain 7.45) and (B) control cells (red gain 7.60) and cells treated with nocodazole (red gain 8.05) for 2 hours. Scale bar = 20µm. Gains were changed here, only, to show more clearly differences in the organisation of the cytoskeleton. The higher gain needed for signal (B) and disorganised structure of the cytoskeletal proteins (A & B) demonstrate successful disruption of actin and tubulin respectively. (C) Treatment with cytochalasin D and nocodazole at 72 hours did not change the percentage of nuclei in SNCs. (D) Addition of cytochalasin D and nocodazole at 40-42 hours did not change the

number of cells syncytialising or (E) the percentage of nuclei in SNCs (n=3). There was also no significant change in number of SNAs in placental explants after treatment with 0.1μM, 1μM or 10μM, (F) cytochalasin D, (G) nocodazole or (H) paclitaxel (n=6) (Kruskal-Wallis test).

Figure 5 – (a) The average size of cluster of which a given nucleus is likely to be a member, as a function of the stickiness parameter S. (b) The average size of cluster of which a given nucleus is likely to be a member, as a function of the diffusion parameter D. (c) The average size of cluster of which a given nucleus is a member, as the preferential sites parameter σ is altered. The distribution of the fusion sites in this experiment is given by a normal distribution with mean L/2 and variance σ^2. (d) The average size of cluster of which a given nucleus is a member, as the amplitude A is altered. (e) Visualisations of a section of the syncytium with two clusters of nuclei (top) and a section with only small clusters (bottom), computed using our model.

Supplementary Images Figure Legends

Supplementary Figure 1 – The potential function that was used as default within the in silico model.

Supplementary Figure 2 – (A) Representative micrographs of SNAs at different time intervals and oxygen concentrations demonstrating tissue changes, such as trophoblast layer shedding (*). SNAs shown by filled arrows. (B) Cytokeratin-7 (green and bottom right) and E-cadherin (red and top left) duel staining surrounding SNAs in fresh tissue and placental explants cultured for: 4 days, 8 days, 12 days and 16 days. Strong cytokeratin-7

staining was seen within and surrounding SNAs throughout the culture period. E-cadherin staining was obvious in fresh tissue but was more difficult to detect from day 8 onwards. Negative control images demonstrate no significant staining. (Scale bar = 20μm; SNAs are indicated with white arrows CTB = cytotrophoblast, FV = fetal vessels).

Supplementary Figure 3 – β-tubulin staining (green) in the region of SNAs in (A) fresh tissue and placental explants cultured for: (B) 4 days, (C) 8 days, (D) 12 days and (E) 16 days. (F) Negative control demonstrates no staining. α-tubulin staining (green) in the region of SNAs is shown in (G) fresh tissue and placental explants cultured for: (H) 4 days, (I) 8 days, (J) 12 days and (K) 16 days. (L) Negative control demonstrates no staining. γ-actin staining (green) in the region of SNAs in (M) fresh tissue and placental explants cultured for: (N) 4 days, (O) 8 days, (P) 12 days and (Q) 16 days. (R) Negative control demonstrates no staining. β-actin staining (green) in the region of SNAs is shown in (S) fresh tissue and placental explants cultured for: (T) 4 days, (U) 8 days, (V) 12 days, and (W) 16 days. (X) Negative control demonstrates no staining. Scale bar represents 20μm, SNAs are indicated with white arrows. STB = syncytiotrophoblast (STB), FV = fetal vessels.

Supplementary Figure 4 – E-cadherin staining (green) of cytotrophoblast cells cultured for (A) 2 days, (B) 4 days and (C) 6 days, highlighting some marked individual cytotrophoblasts (*), syncytia (yellow S) and apoptosed syncytia with condensed nuclei (white arrows).

Supplementary Figure 5 – Representative images of actin immunofluoresence staining (green) in (A) DMSO treated (vehicle control) explants; and explants treated with (B) 10μM and (C) 0.1μM cytochalasin D. The long filamentous actin in control tissue has been

interrupted by cytochalasin D treatment which shows globular, punctate staining. Representative images of tubulin staining in placental explants treated with (D) DMSO (vehicle control); (E) 10μM, (F) 0.1μM nocodazole, (G) 10μM (H) 0.1μM paclitaxel. There was loss of staining in nocodazole treated explants compared to the DMSO control and stabilised tubulin in the paclitaxel treated explants. Scale bar =20μm.

Supplementary Table 1 - Demographic data for participants whose placentas were used in this study.

Supplementary Table 2 - The parameters from the potential function for the in silico model, with the values they hold.

Supplementary Table 3 - EST numbers of SUN and SYNE proteins in human placenta.

Supplementary videos

Supplementary video 1 (Day 0 to 1) - Cells were plated out and starting at 3 h of culture they were imaged every 10 min for 104 images. It is possible to see the cells initially start in tightly clustered balls and then spread out to cover a larger proportion of the field of view (labelled in one area by a red circle, which enlarges as the cells spread out). Later in the video the location of three nuclei become visible (annotated by three*). Recorded using x 10 lens, no magnifier. Diameter of circle on still image= 115 μm.

Supplementary video 2 (Day 2 to 3) – Unfused cells were plated out and at 48 h of culture the cell clusters were imaged every 5 min for 180 images. It is possible to see the

cell membrane movement in this video annotated by red lines to show a large movement (middle right line) and smaller movements (top line) but the nuclei do not move much at all, three of which are labelled by*. Occasionally cells can be seen undergoing apoptosis two of which are labelled (A and B). Red scale bar= 55 µm.

Supplementary video 3 (Day 4 to 5) - Cells were plated out and at 96 h of culture they were imaged every 10 min for 104 images. There is little movement of the cell membranes noted during this time frame and nuclei do not appear to move (two of which are labelled by *), although fibroblast cells can be seen moving around the syncytium (within the red circle). Later in the video a syncytium at the top of the video undergoes apoptosis (labelled A) Scale bar= 69 µm.

Supplementary video 4 (Cytochalasin D treated) - Cells were plated out and at 72 h of culture they were imaged every 5 min for 280 images. A cluster of nuclei is highlighted with a red circle and two nuclei within that group are marked * which tracks the movements of those nuclei. The cell membrane in this video appears to shrink and to draw closer together and the nuclei also appear to move in association with the cell membrane movements. The fibroblast in the top right corner does not move much, in contrast to the fibroblast in supplementary video 3 implying that cytochalasin D has been effective in inhibiting actin remodelling, furthermore after 3 seconds of video the fibroblast begins to round. Disrupting actin polymerisation does not appear to cause nuclear clusters to separate, but may affect cell shape and through that may indirectly cause small nuclear movements. Scale bar= 36 µm.

Supplementary video 5 (Nocodazole treated) -Cells were plated out and at 72 h of culture they were imaged every 5 min for 213 images. It is possible to see the cells bunch up, unable to retain their shape (annotated by two red lines that move closer to each other throughout the video); the nuclei move to accommodate changes in the position of the cell membrane (two of which have their movements labelled* for clarity), but nuclei do not move relative to other nuclei. The fibroblasts in the lower right corner bleb more and have less directed movement implying that nocodazole has been effective in inhibiting tubulin remodelling. Disrupting tubulin polymerisation does not appear to cause nuclear clusters to separate, but may affect cell shape and through that may indirectly cause nuclear movements. Scale bar= 45.5µm.

Supplementary video 6 (both cytochalasin D and nocodazole treated) - Cells were plated out and at 72 h of culture they were imaged every 5 min for 180 images. In the bottom left corner a syncytium appears to move away from the other more central area of syncytium (shown by an annotated red line that moves off screen as the cell membrane also moves off screen). Two nuclei are marked by * and the nucleus in the top syncytium does not appear to move whereas the nucleus in the lower syncytium moves with cell membrane movements. Scale bar= 27 µm.

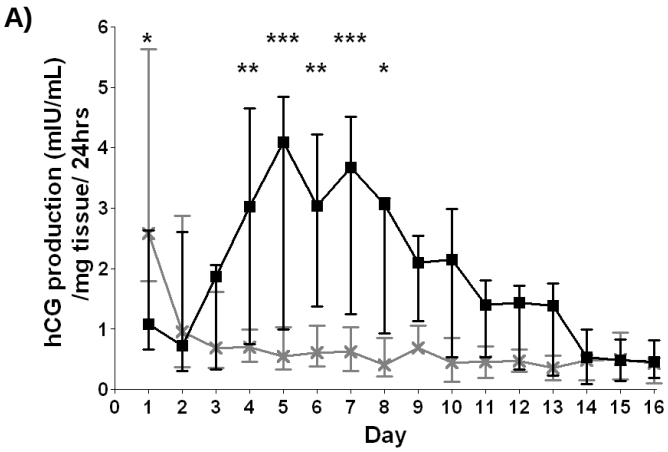
A)
hCG production (mIU/mL) /mg tissue/ 24hrs
Day

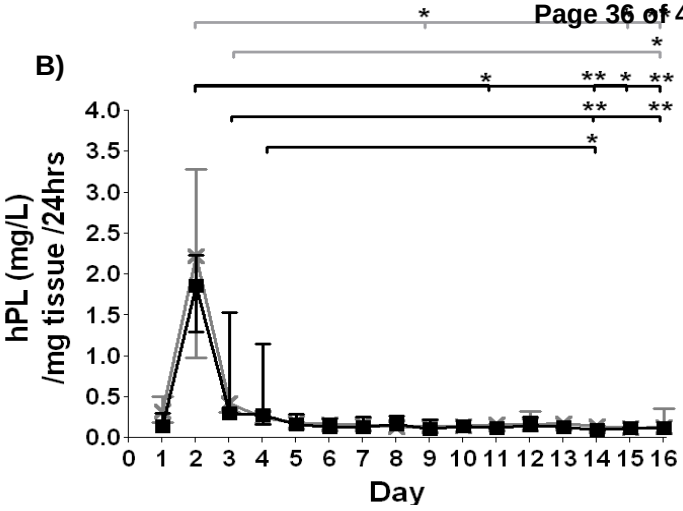
B)
hPL (mg/L) /mg tissue /24hrs
Day

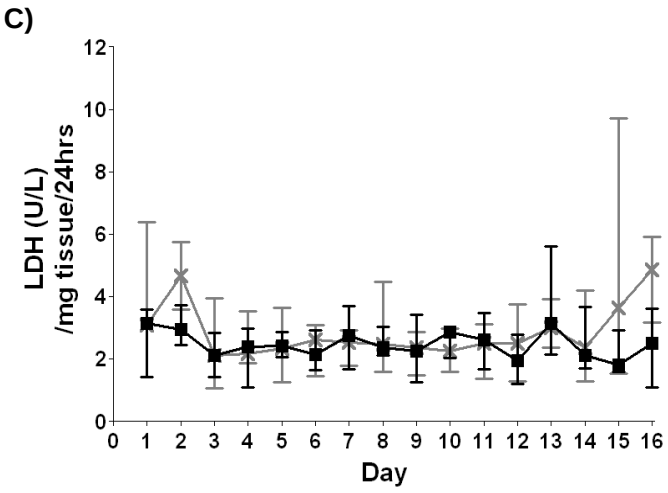
C)
LDH (U/L) /mg tissue/24hrs
Day

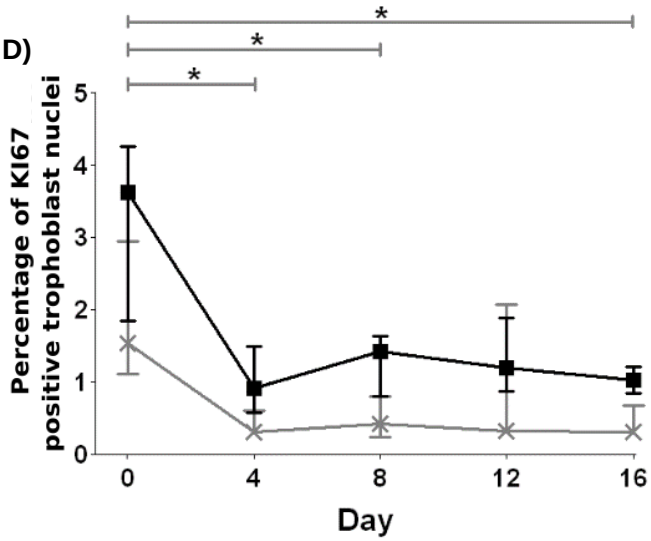
D)
Percentage of KI67 positive trophoblast nuclei
Day

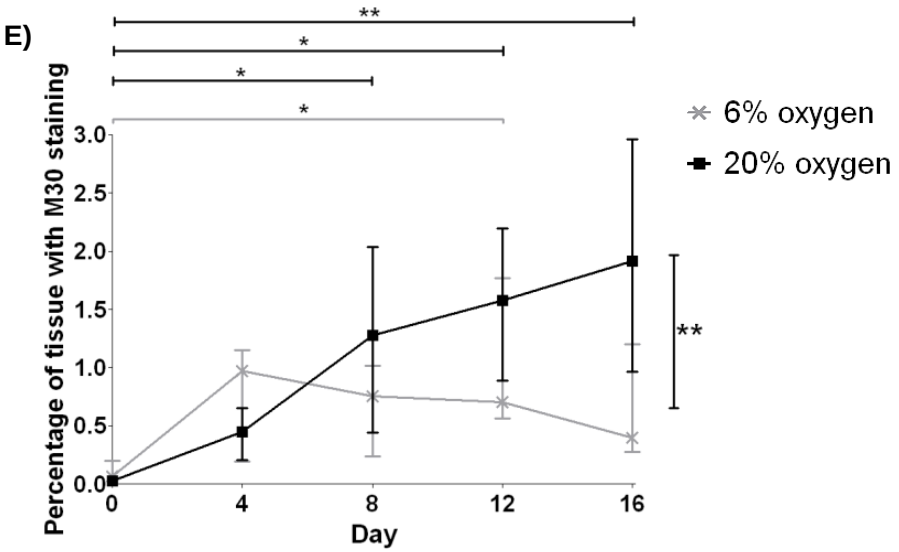
E)
Percentage of tissue with M30 staining
6% oxygen
20% oxygen
Day

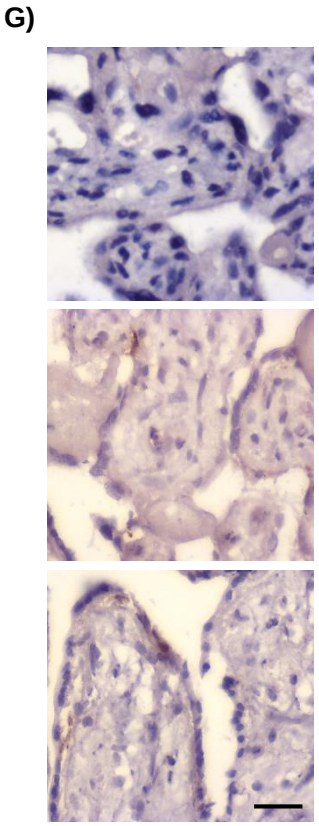
G)
Day 0
Day 8
Day 16

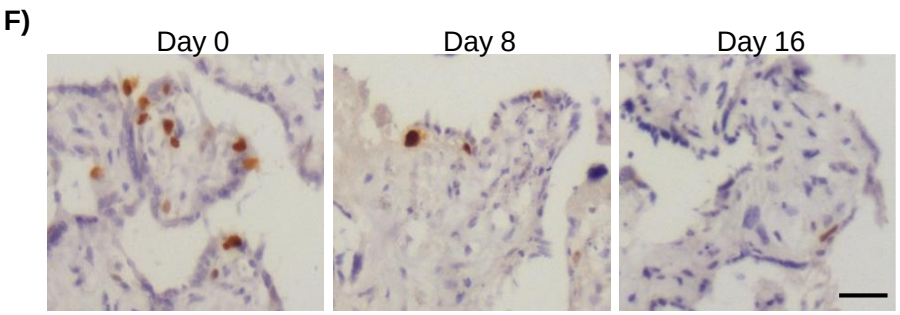
F)
Day 0
Day 8
Day 16

A)

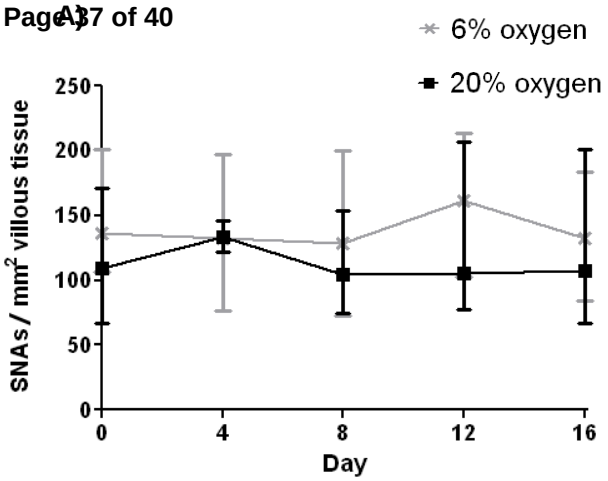
6% oxygen
20% oxygen
SNAs / mm² villous tissue
Day

B)

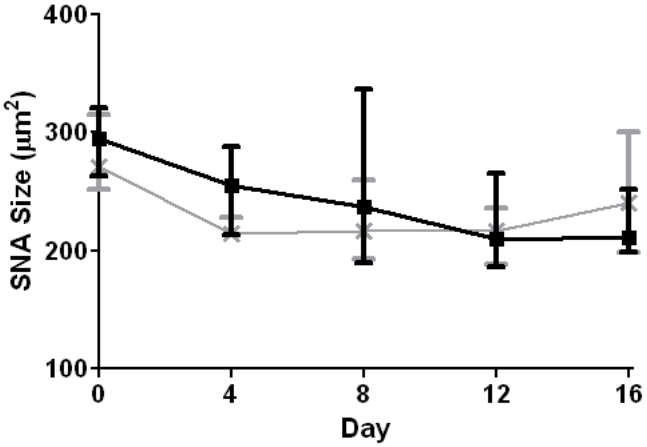
SNA Size (µm²)
Day

C)

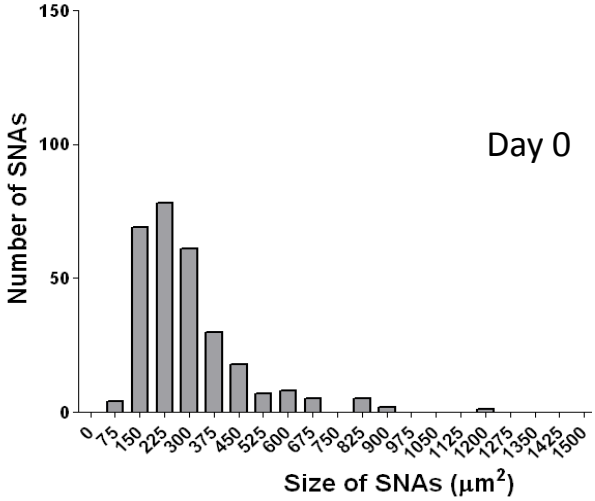
Day 0
Number of SNAs
Size of SNAs (µm²)

D)

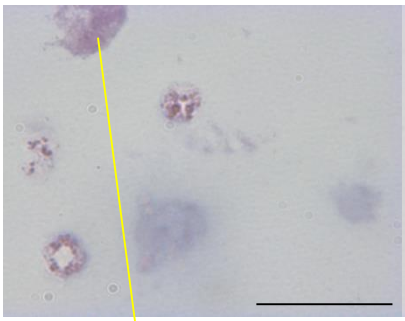
Individual cells
cytoplasm

E)

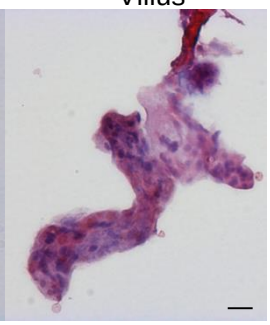
Villus

F)

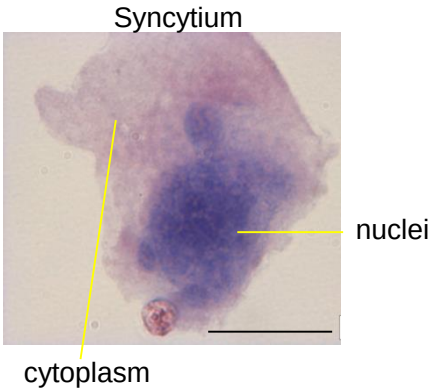
Syncytium
nuclei
cytoplasm

G)

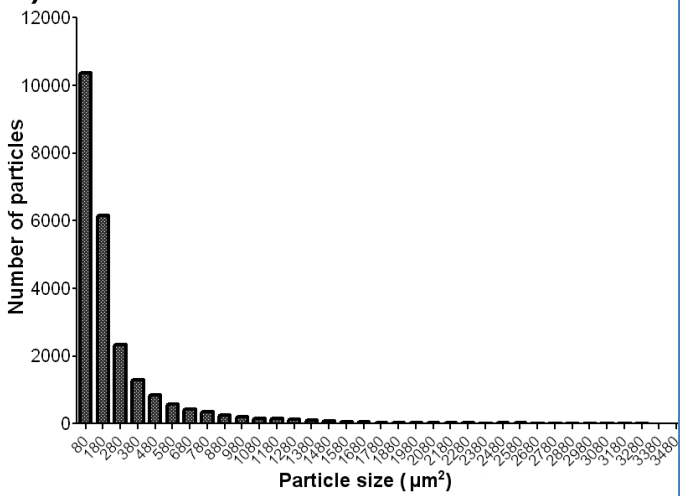
Number of particles
Particle size (µm²)

H)

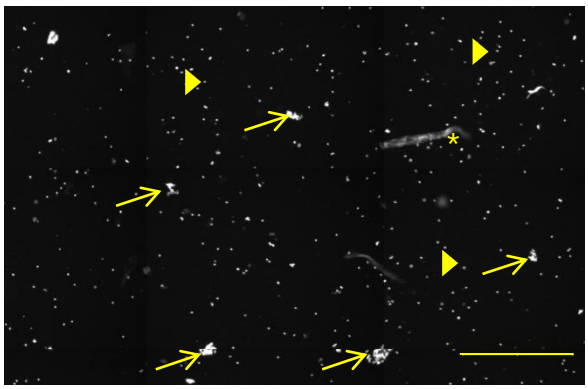

I)

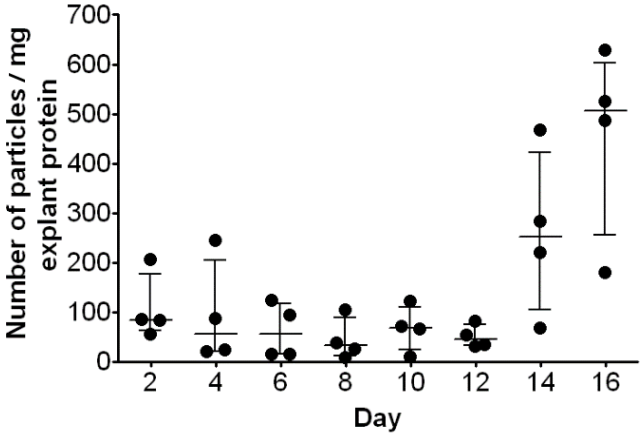
Number of particles / mg explant protein
Day

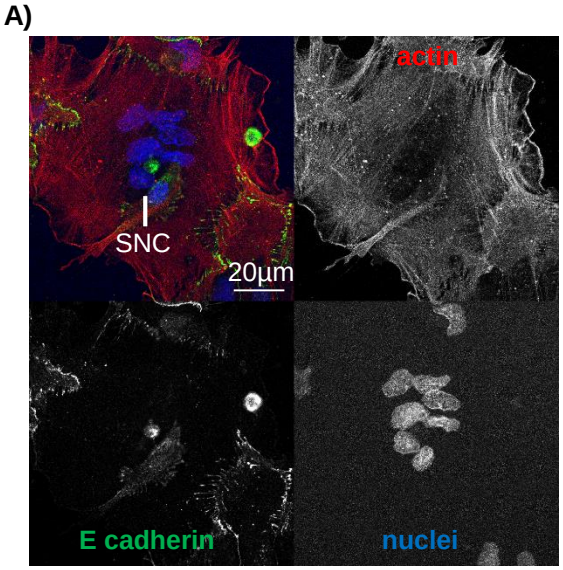
A)
actin
SNC
20µm
E cadherin
nuclei

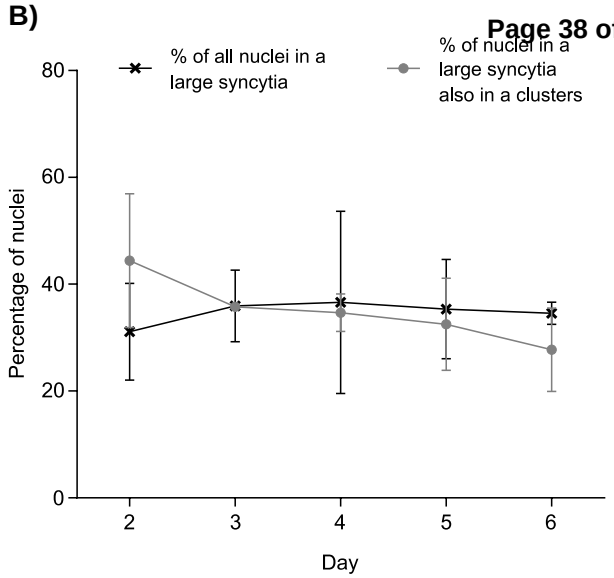
B)
% of all nuclei in a large syncytia
% of nuclei in a large syncytia also in a clusters
Percentage of nuclei
Day

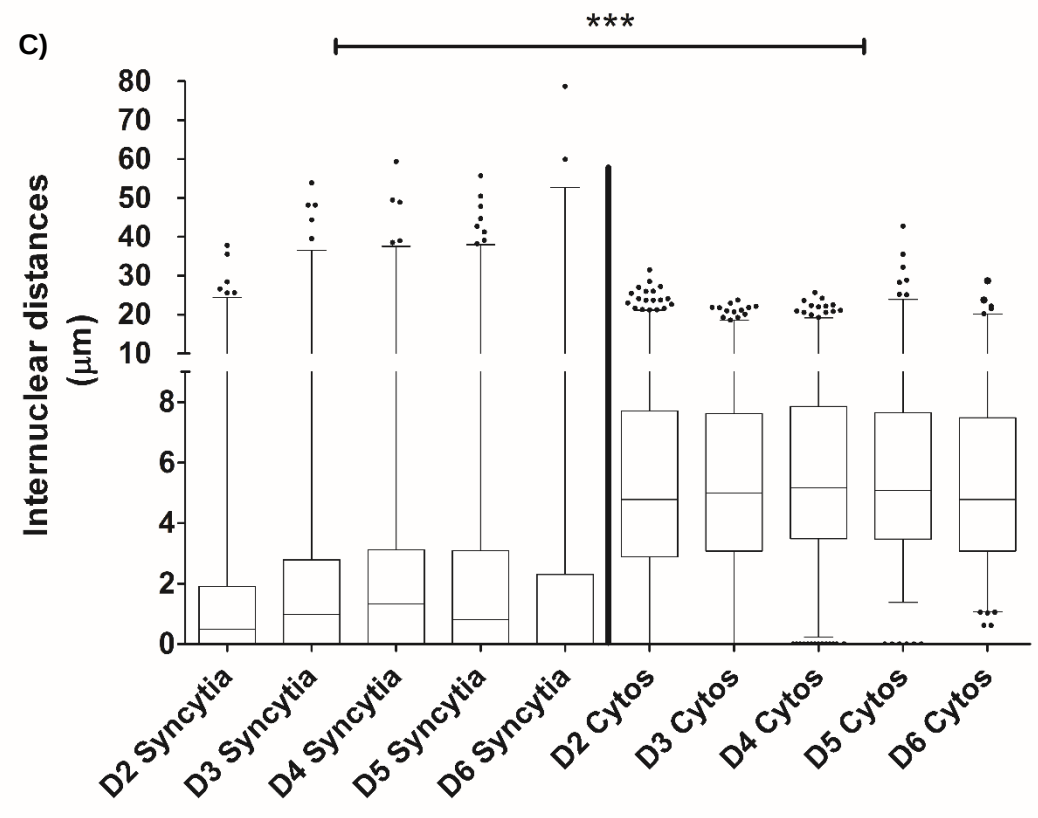
C)
***
Internuclear distances (µm)
D2 Syncytia
D3 Syncytia
D4 Syncytia
D5 Syncytia
D6 Syncytia
D2 Cytos
D3 Cytos
D4 Cytos
D5 Cytos
D6 Cytos

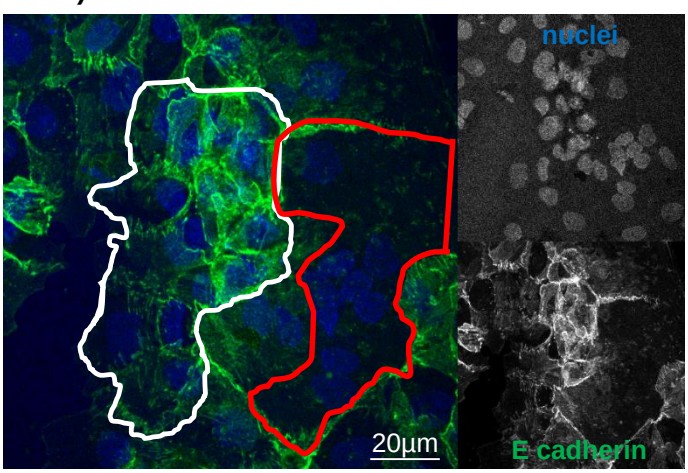
D)
nuclei
20µm
E cadherin

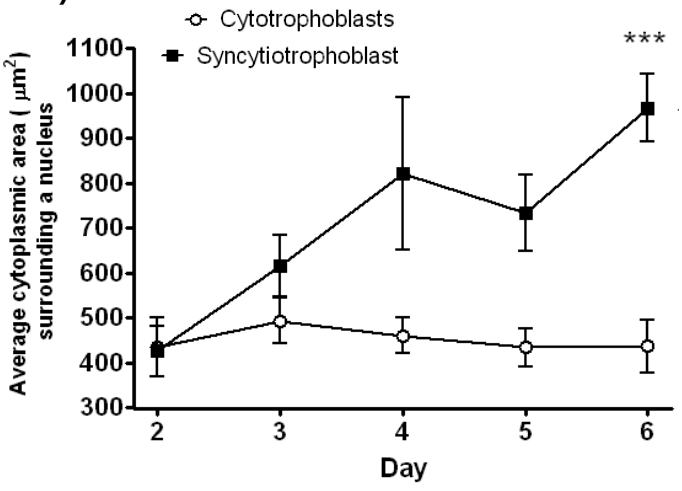
E)
Cytotrophoblasts
Syncytiotrophoblast
***
Average cytoplasmic area (µm²) surrounding a nucleus
Day

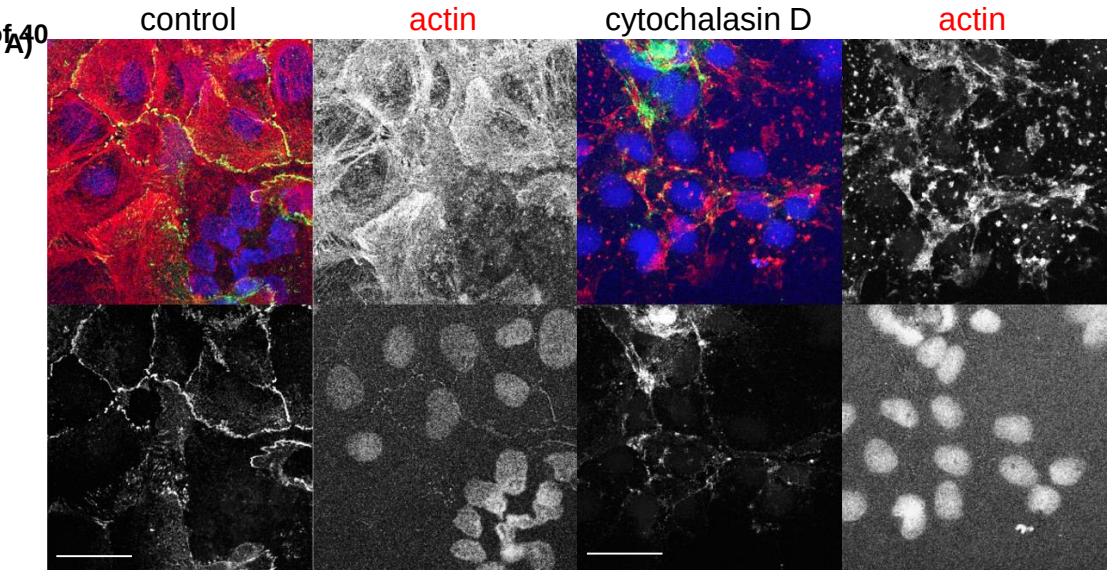
A)
control
actin
cytochalasin D
actin
E cadherin
nuclei
E cadherin
nuclei

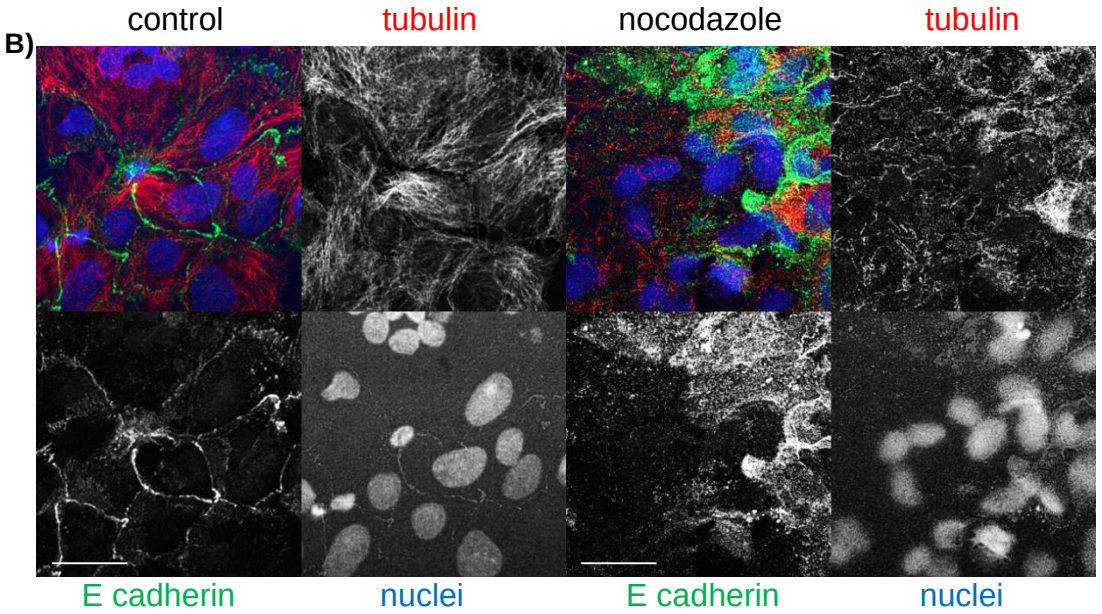
B)
control
tubulin
nocodazole
tubulin
E cadherin
nuclei
E cadherin
nuclei

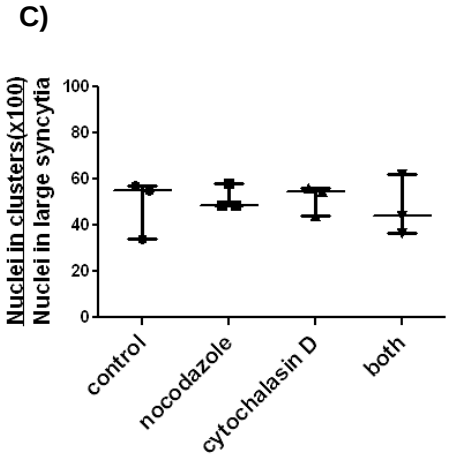
C)
Nuclei in clusters(x100)
Nuclei in large syncytia
control
nocodazole
cytochalasin D
both

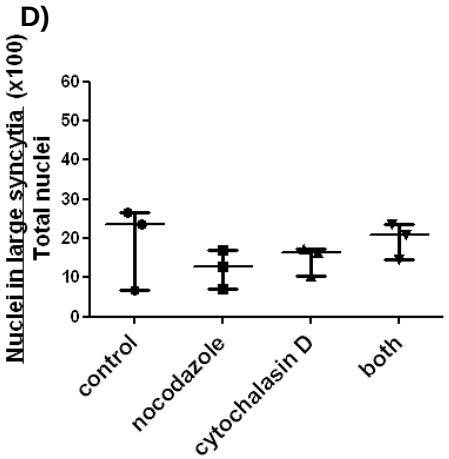
D)
Nuclei in large syncytia (x100)
Total nuclei
control
nocodazole
cytochalasin D
both

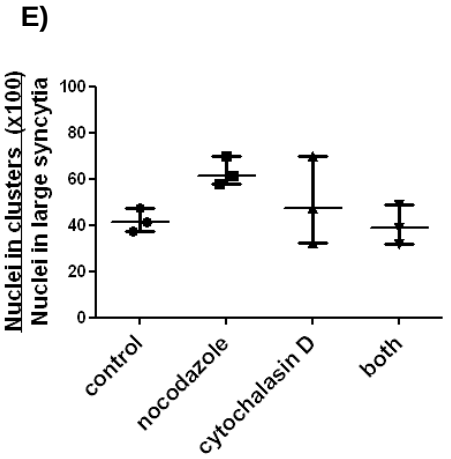
E)
Nuclei in clusters (x100)
Nuclei in large syncytia
control
nocodazole
cytochalasin D
both

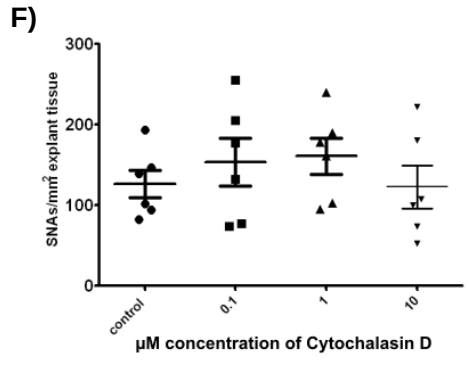
F)
SNAs/mm² explant tissue
control
0.1
1
10
μM concentration of Cytochalasin D

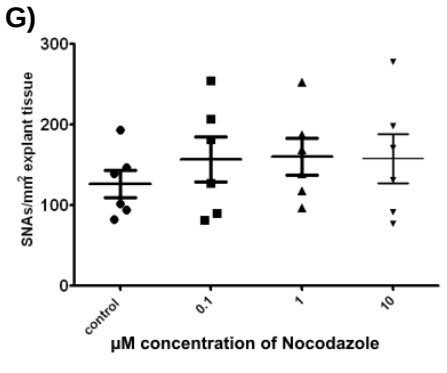
G)
SNAs/mm² explant tissue
control
0.1
1
10
μM concentration of Nocodazole

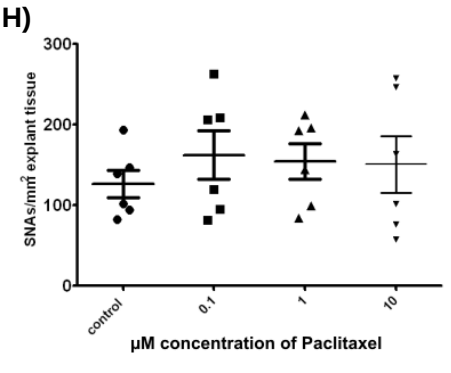
H)
SNAs/mm² explant tissue
control
0.1
1
10
μM concentration of Paclitaxel

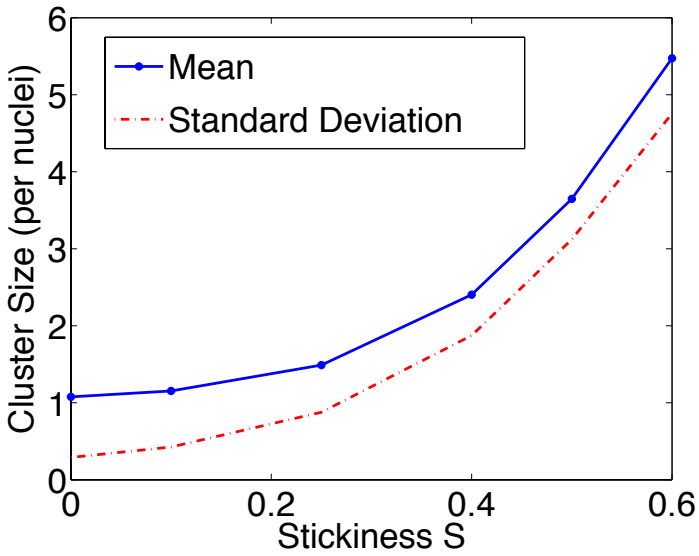
Mean
Standard Deviation
Cluster Size (per nuclei)
Stickiness S
0
1
2
3
4
5
6
0
0.2
0.4
0.6

(a)

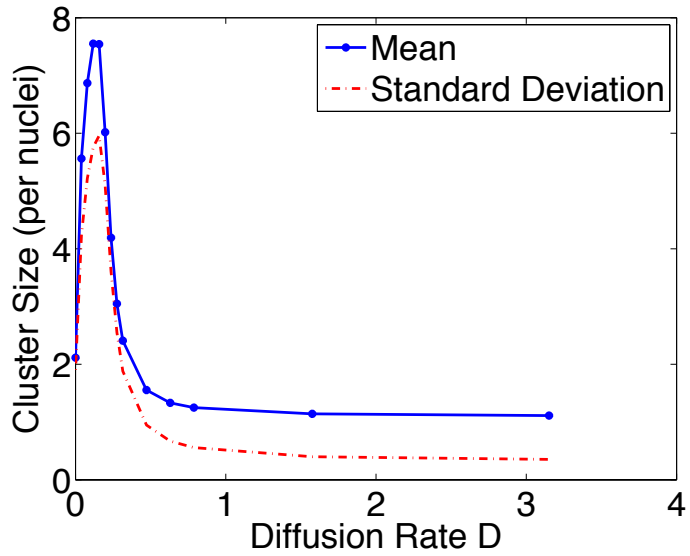
Mean
Standard Deviation
Cluster Size (per nuclei)
Diffusion Rate D
0
2
4
6
8
0
1
2
3
4

(b)

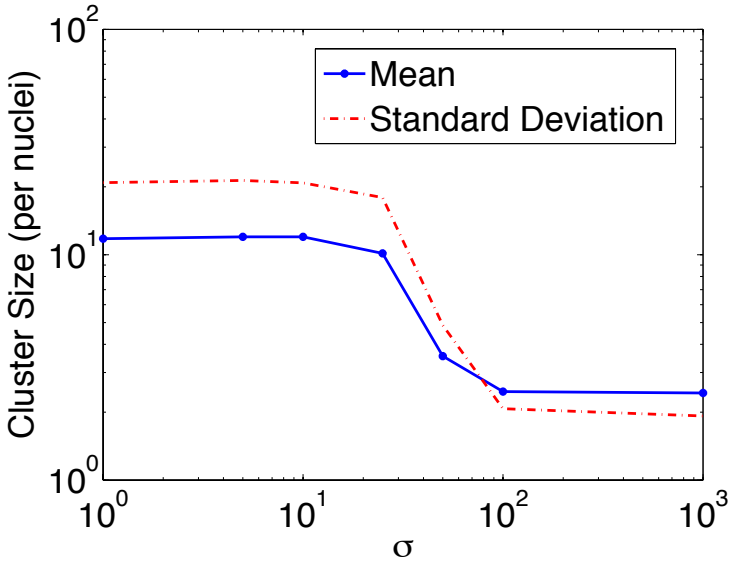
Mean
Standard Deviation
Cluster Size (per nuclei)
σ
10^0
10^1
10^2
10^3

(c)

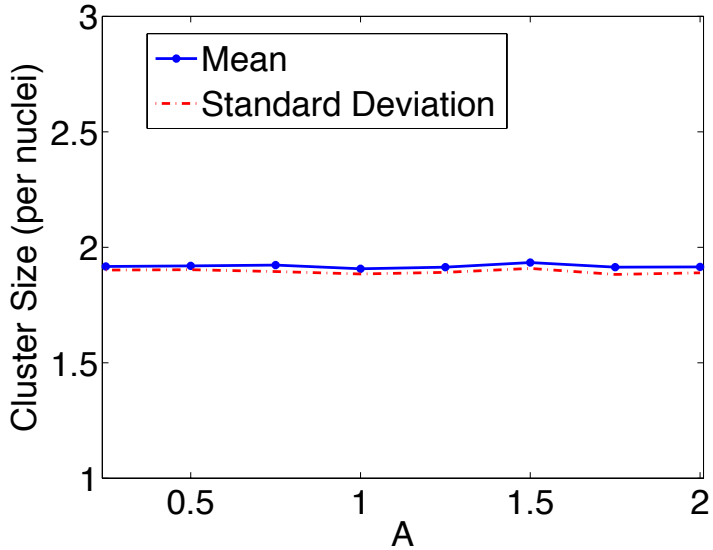
Mean
Standard Deviation
Cluster Size (per nuclei)
A
1
1.5
2
2.5
3
0.5
1
1.5
2

(d)

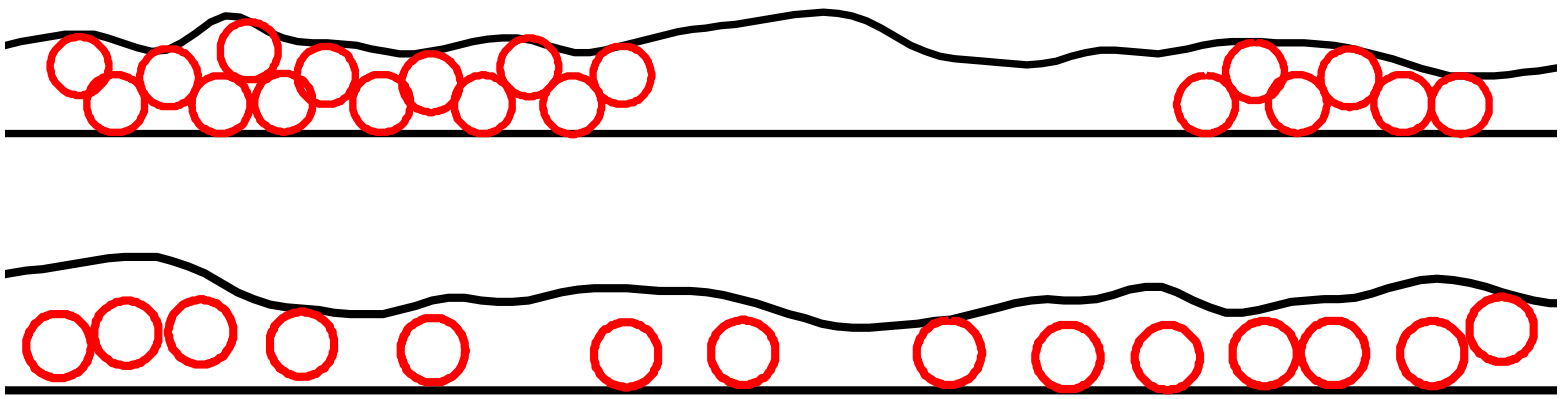

(e)